Smart Structures and Systems, *Vol. 34, No. 2 (2024) 97-116*
https://doi.org/10.12989/sss.2024.34.2.097

l_p-norm regularization for impact force identification from highly incomplete measurements

Yanan Wang [1,2], Baijie Qiao*[1,2], Jinxin Liu [1,2], Junjiang Liu [1,2] and Xuefeng Chen [1,2]

[1] *National Key Lab of Aerospace Power System and Plasma Technology, Xi'an Jiaotong University, Xi'an, 710049, P.R. China*
[2] *School of Mechanical Engineering, Xi'an Jiaotong University, Xi'an, 710049, P.R. China*

(*Received June 3, 2022, Revised September 1, 2024, Accepted September 23, 2024*)

Abstract. The standard l_1-norm regularization is recently introduced for impact force identification, but generally underestimates the peak force. Compared to l_1-norm regularization, l_p-norm $(0 \leq p < 1)$ regularization, with a nonconvex penalty function, has some promising properties such as enforcing sparsity. In the framework of sparse regularization, if the desired solution is sparse in the time domain or other domains, the under-determined problem with fewer measurements than candidate excitations may obtain the unique solution, i.e., the sparsest solution. Considering the joint sparse structure of impact force in temporal and spatial domains, we propose a general l_p-norm $(0 \leq p < 1)$ regularization methodology for simultaneous identification of the impact location and force time-history from highly incomplete measurements. Firstly, a nonconvex optimization model based on l_p-norm penalty is developed for regularizing the highly under-determined problem of impact force identification. Secondly, an iteratively reweighed l_1-norm algorithm is introduced to solve such an under-determined and unconditioned regularization model through transforming it into a series of l_1-norm regularization problems. Finally, numerical simulation and experimental validation including single-source and two-source cases of impact force identification are conducted on plate structures to evaluate the performance of l_p-norm $(0 \leq p < 1)$ regularization. Both numerical and experimental results demonstrate that the proposed l_p-norm regularization method, merely using a single accelerometer, can locate the actual impacts from nine fixed candidate sources and simultaneously reconstruct the impact force time-history; compared to the state-of-the-art l_1-norm regularization, l_p-norm $(0 \leq p < 1)$ regularization procures sufficiently sparse and more accurate estimates; although the peak relative error of the identified impact force using l_p-norm regularization has a decreasing tendency as p is approaching 0, the results of l_p-norm regularization with $0 \leq p \leq 1/2$ have no significant differences.

Keywords: impact force identification; l_1-norm regularization; l_p-norm regularization; nonconvex optimization; sparse regularization; under-determined system

1. Introduction

The knowledge of impact force location and time-history is of great significance for assessing the structural integrity in structural health monitoring (Mahzan *et al*. 2010, Yan *et al*. 2017, Chen *et al*. 2018, Zhong and Xiang 2019). For example, external object impacts such as the drop of ice hails or maintenance tools, may induce internal damages to aerospace structures during their long-term service life. However, the direct measurement of impact forces is infeasible, because the insertion of force gages into impact locations is extremely challenging. Consequently, an indirect estimation of external impact forces from output responses has been attempted, which is a typical inverse problem. Like other inverse problems in structural dynamics, impact force identification might be inherently ill-conditioned, which means that even small variations in the measured response may cause large fluctuations in the force estimation. In this context, it does not necessarily have a unique and stable solution when noisy and limited measurements are used.

Impact force identification includes the localization of impact events and the reconstruction of the force time-history. Inoue *et al*. (2001) presented a literature review of inverse techniques for localization and reconstruction of impact forces. The mostly used regularization methods are the truncated singular value decomposition (TSVD) method and Tikhonov regularization method, the latter of which is also known as l_2-norm regularization. There generally exist over-determined, even-determined and under-determined problems in impact force identification. Given the localization of forces, Thite and Thompson (2003) applied TSVD and Tikhonov regularization for identifying the forces acting on the plate under over-determination in the frequency domain. When the impact location is known, Jacquelin *et al*. (2003) used Tikhonov regularization and TSVD for reconstructing the impact force history under even-determination in the time domain. Qiao *et al*. (2016b) respectively applied Daubechies wavelets and cubic B-spline functions to approximate the profile of the impact force under even determination. Saleem and Jo (2019) proposed the augment Kalman filter for impact localization and then used genetic algotrithm to construct the force time history. Khoo *et al*. (2014) discussed three configurations,

*Corresponding author, Ph.D., Professor,
E-mail: qiao1224@xjtu.edu.cn

http://www.techno-press.org/?journal=sss&subpage=7
ISSN: 1738-1584 (Print), 1738-1991 (Online)

under-determined, even-determined and over-determined cases of localizing and simultaneously reconstructing impact force in the frequency domain. Khoo's experiments showed that for the under-determined case with fewer measurements than possible impacts, all response combinations (two, four and five accelerometers) failed to reconstruct the time-history of impact force and led to the false localization of impacts. Therefore, solving the undetermined problem where the number of measurements is less than that of possible excitations, poses a severe challenge to existing regularization algorithms.

This paper focuses on a highly under-determined problem of impact force identification: simultaneous localization and reconstruction of impact forces, where the number of candidate impacts is greatly more than the number of measurements. For an under-determined linear system with fewer equations than unknowns, intuitively, there exist infinitely many solutions. Sparse regularization by considering the sparsity prior of impact force could generate the sparsest solution to approximate the exact solution of the under-determined system of impact force identification. The widely used sparse regularization method in inverse problem community is Lasso regularization, in which the penalty term is l_1-norm instead of l_2-norm (Donoho 2006). Some more recent work in impact force identification has focused on sparse regularization based on l_1-norm penalty (Qiao *et al.* 2016a, 2017, 2020b, Pan *et al.* 2018, Li and Lu 2018, Wambacq *et al.* 2019). Qiao *et al.* (2016a) presented an impact force sparse reconstruction method based on l_1-norm penalty using highly incomplete and inaccurate measurements, where only one accelerometer was employed to identify one or two impact forces from a total of nine possible locations. However, l_1-norm regularization may yield underestimated solutions and show limited identification ability when only few measurements are available for impact force identification. However, sparse regularization methods based on the l_1 norm usually underestimate the magnitude of the impact force and yield erroneous impact force identification results (Selesnick and Bayram 2014, Qiao *et al.* 2020a). Hence, nonconvex sparse regularization is considered to ameliorate this problem (Liu *et al.* 2023). Some nonconvex sparse regularization methods have been studied for impact force identification (Liu *et al.* 2020, Zhou *et al.* 2024). Chartrand (2007) introduced the nonconvex compressive sensing, where the standard l_1-norm is replaced with l_p-norm ($0 < p < 1$). Subsequently, numerical experiments showed that l_p-norm minimization manages to recover sparse signals from substantially fewer measurements than l_1-norm minimization does (Chartrand 2007). The general l_p-norm penalty with $0 < p < 1$ is considered to enhance the crucial features of l_1-norm regularization and approximate l_0-norm regularization. Different from the l_1-norm, which is a convex relaxation of the l_0-norm, the l_p-norm ($0 < p < 1$) as an interpolation between the l_0-norm and l_1-norm fills the gap between the two. Therefore, the regularization method based on the l_p-norm ($0 < p < 1$) can achieve sparser solutions compared to the l_1-norm, enhancing the recovery of sparse vectors in the inverse problem.

Inspired by the great success of l_p-norm ($0 < p < 1$) regularization in the inverse problem community and considering the sparsity nature of the impact force in temporal and spatial domains, this paper proposes a nonconvex sparse regularization model based on l_p-norm ($0 < p < 1$) penalty for impact force identification. The main contributions of this paper are as follows. The standard l_1-norm regularization is extended to the nonconvex l_p-norm regularization for improving the sparsity and accuracy of impact force identification from highly incomplete measurements. The performance of l_p-norm regularization with arbitrary p values ($0 \le p \le 1$) in locating and simultaneously reconstructing time-history of impact force identification is evaluated. The iteratively reweighted l_1-norm minimization (IRL1) (Candes *et al.* 2008) which was proposed to enhance the sparsity of l_1-norm minimization is here developed to solve the unconditioned l_p-norm regularization of impact force inverse problem from highly incomplete measurements. The unique solution of the under-determined problem of impact force identification is achieved by a sufficiently sparse solution of l_p-norm regularization. l_p-norm regularization for impact force identification proposed in this paper and tackled by IRL1 algorithm is easier to be solved than l_0-norm regularization and, meanwhile, generates much sparser and more accurate solutions than l_1-norm regularization does.

The paper is organized as follows. In Section 2, the general formulation of impact force identification problems is formulated and the under-determined system is analyzed. In Section 3, we outline l_p-norm ($0 \le p \le 1$) regularization strategies including the standard sparse regularization and nonconvex sparse regularization models, and discuss their difference. In Section 4, an iteratively reweighted l_1-norm minimization algorithm is derived for solving the unconditioned l_p-norm regularization model of under-determined problems of impact force identification, in which a standard l_1-norm regularization problem is solved at each iteration. In Section 5 and Section 6, numerical and experimental validations including single-source and two-source cases of impact force identification from highly incomplete measurements are conducted to demonstrate the advantage of l_p-norm regularization over l_1-norm regularization. Conclusions are given in Section 7.

2. General formulation of impact force identification

For a linear time-invariant mechanical system, when the impact location is known, the output response $y_i(t)$ at point i relates to the input force $f_j(t)$ at point j and the impulse response function $h_{ij}(t)$, defined by the convolution integral form as follows

$$y_i(t) = h_{ij}(t) * f_j(t) = \int_0^t h_{ij}(t-\tau) f_j(\tau) d\tau \qquad (1)$$

where $*$ represents the convolution operator, and τ is the time delayed operator satisfying $t \ge \tau$. $h_{ij}(t)$ gives a mathematical representation of the relationship between the output response and input force in the time domain, which completely describes the dynamic characteristics of the system. Since the forward impact problem can be formulated as a convolution of the impact force and the impulse response function, the deconvolution is considered as straightforward to reconstruct the impact force.

In order to solve the inverse problem of impact force identification, the continuum in Eq. (1) an be discretized as algebraic equations on the time interval $[0, t]$

$$\begin{bmatrix} y_i(\Delta t) \\ y_i(2\Delta t) \\ \vdots \\ y_i((n-1)\Delta t) \\ y_i(n\Delta t) \end{bmatrix} = \Delta t \begin{bmatrix} h_{ij}(\Delta t) & 0 & \cdots & 0 & 0 \\ h_{ij}(2\Delta t) & h_{ij}(\Delta t) & \cdots & 0 & 0 \\ \vdots & \vdots & \cdots & \vdots & \vdots \\ h_{ij}((n-1)\Delta t) & h_{ij}((n-2)\Delta t) & \dots & h_{ij}(\Delta t) & 0 \\ h_{ij}(n\Delta t) & h_{ij}((n-1)\Delta t) & \dots & h_{ij}(2\Delta t) & h_{ij}(\Delta t) \end{bmatrix} \begin{bmatrix} f_j(\Delta t) \\ f_j(2\Delta t) \\ \vdots \\ f_j((n-1)\Delta t) \\ f_j(n\Delta t) \end{bmatrix} \quad (2)$$

where n is the data length and Δt is the time step, namely the sampling interval. The sampling frequency $f_s = \frac{1}{\Delta t}$ depends on the working frequency range of interest. As a consequence, it is convenient to express the convolution problem of Eq. (2) in a matrix-vector form as

$$\boldsymbol{y}_i = \boldsymbol{H}_{ij}\boldsymbol{f}_j \quad (3)$$

where $\boldsymbol{y}_i \in \boldsymbol{R}^{n\times 1}$ is the measured response vector, $\boldsymbol{f}_j \in \boldsymbol{R}^{n\times 1}$ is the impact force vector to identify, and the lower triangular Toeplitz matrix $\boldsymbol{H}_{ij} \in \boldsymbol{R}^{n\times n}$ is the transfer function matrix. One can cast the deconvolution problem of inferring the input force $\boldsymbol{f}_j$ from the output response $\boldsymbol{y}_i$ as a linear inverse problem, the purpose of which is to solve Eq. (3). The response signal $\boldsymbol{y}_i$ can be experimentally measured as any of physical quantities—displacement, velocity, acceleration, or strain. The impact force signal $\boldsymbol{f}_j$ is generally sparse in the time domain $[0, t]$, relative to its size. Eq. (3) describes a forward problem of a single-input-single-output (SISO) system.

In many practical situation, multiple impact forces rather than a single impact event impose in finite locations. For the inverse problem of the multiple-source impact force identification, several unknown forces act on different locations over a structure and several responses are synchronously recorded over a small time period. Here, the governing equation of such a multiple-input multiple-output (MIMO) system can be expressed in a matrix form.

$$\begin{bmatrix} \boldsymbol{y}_1 \\ \boldsymbol{y}_2 \\ \vdots \\ \boldsymbol{y}_M \end{bmatrix} = \begin{bmatrix} \boldsymbol{H}_{11} & \boldsymbol{H}_{12} & \cdots & \boldsymbol{H}_{1N} \\ \boldsymbol{H}_{21} & \boldsymbol{H}_{22} & \dots & \boldsymbol{H}_{2N} \\ \vdots & \vdots & \ddots & \vdots \\ \boldsymbol{H}_{M1} & \boldsymbol{H}_{M1} & \cdots & \boldsymbol{H}_{MN} \end{bmatrix} \begin{bmatrix} \boldsymbol{f}_1 \\ \boldsymbol{f}_2 \\ \vdots \\ \boldsymbol{f}_N \end{bmatrix} \quad (4)$$

where *M* is the number of the measurement sensors, and *N* is the number of possible impact forces to be identified. Submatrix $\boldsymbol{H}_{ij}$ is the transfer function matrix between the measured point i and the impact located point j. Each response vector $\boldsymbol{y}_i$ corresponds to a measurement sensor and each force vector $\boldsymbol{f}_j$ corresponds to a possible excitation source. In general, for the purpose of impact localization, the number of candidate locations is much larger than the number of the actual impact sources. In such a circumstance, the actual impact sources can be determined from *N* candidate locations via regularization methods.

For simplicity, the input-output relation in Eq. (4) can be expressed as a matrix-vector form

$$\boldsymbol{y} = \boldsymbol{H}\boldsymbol{f} \quad (5)$$

where the rewritten transfer matrix $\boldsymbol{H} \in \mathbb{R}^{nM\times nN}$ is a Toeplitz block matrix. The force vector $\boldsymbol{f} = [\boldsymbol{f}_1, \boldsymbol{f}_2, \dots, \boldsymbol{f}_N]^T \in \boldsymbol{R}^{nN\times 1}$ is the collection of all the possible impact forces, and the response vector $\boldsymbol{y} = [\boldsymbol{y}_1, \boldsymbol{y}_2, \dots, \boldsymbol{y}_N]^T \in \boldsymbol{R}^{nM\times 1}$ is a multi-channel vector consisting of *M* measurements.

In practice, the measured response is rarely noiseless. This noisy distortion is often modeled by a perturbation vector $\boldsymbol{e}$ as follows

$$\boldsymbol{y} = \boldsymbol{H}\boldsymbol{f} + \boldsymbol{e} \quad (6)$$

In this work, the goal of impact force identification is to solve Eq. (6) for determining the multiple impact locations and simultaneously reconstructing the time-history of *N* assumed impact forces. In many situations, the transfer function matrix is too ill-conditioned (even rank-deficient) to allow a numerically stable and unique solution. Even a small perturbation in the measured data may cause a considerable change in $\boldsymbol{f}$. In order to overcome the ill-posed nature of impact force identification, the number of measurement sensors is required to be larger than the number of candidate excitations in existing references (Thite and Thompson 2003). When multiple sensors are available, the pseudo-inverse method can be directly implemented to solve such an over-determined linear system in Eq. (6) for a stable solution. In this context, the pseudo-inverse method provides some redundancy by utilizing response measurements at extra locations to reduce the measurement error and thereby improves the accuracy of the identified forces. This approach results in estimated forces that are usually distributed over the whole structure (Park *et al.* 2009, Kalhori *et al.* 2018).

However, more sensors may not be allowed and are not economical. As for the MIMO system, the inverse problem of impact force identification can be divided into three categories depending on the relationship between the number of responses and the number of assumed impact locations:

(I) Over-determined case (*M* > *N*): the number of measurements is larger than that of candidate excitations.
(II) Even-determined case (*M* = *N*): the number of measurements is equal to that of candidate excitations.
(III) Under-determined case (*M* < *N*): the number of

measurements is smaller than that of candidate excitations.

Here, we are primarily concerned with the under-determined case of impact force identification including impact localization and force history reconstruction. Assuming the number of actual impact forces is small, the impact distribution is sparse in space. Furthermore, it is assumed that each impact force vector $\boldsymbol{f}_j$ is localized in the time axis. Therefore, once the unknown excitation field is exactly reconstructed, impact force can be simultaneously localized. Here, we are particularly interested in the special case where only a single accelerometer is available and nine candidate sources over the entire structure are selected. Therefore, we are facing a severely under-determined and large-scale ill-posed problem. The challenge now is to develop efficient regularization methods to solve such an under-determined inverse problem. The useful prior characteristic is the jointly sparse nature of impact force in temporal and spatial domains, which has only a small number of nonzero components around the peak force compared to its dimension.

3. l_p-norm regularization for impact force identification

We want to reconstruct high-dimensional sparse impact-force vectors from low-dimensional measurements. This difficulty can be managed by the so-called sparsity-promoting regularization, which involves applying additional constraints as a prior to regularize the inverse problem to obtain a stable and unique solution. The underlying information of impact force identification is that the force time-history is sufficiently sparse and the distribution of limited impact forces is also sparse in the spatial domain. Hence, it is possible to solve the under-determined problem of impact force identification with its inherent sparsity by sparse regularization from fewer measurements than possible excitations. As a result, finding the unique solution of under-determined problem absolutely turns into the search of the sparsest solution.

A natural approach is to find the sparsest solution of the general under-determined problem of impact force identification by solving the following l_0-norm minimization problem.

$$\underset{\boldsymbol{f}}{\text{minimize}}\{\|\boldsymbol{f}\|_0 : \boldsymbol{y} = \boldsymbol{H}\boldsymbol{f}\} \tag{7}$$

where the l_0-norm $\|\cdot\|_0$ simply counts the number of nonzero components in a vector. Hence, l_0-norm minimization corresponds to making as many as possible entries in $\boldsymbol{f} \in \boldsymbol{R}^{nN\times 1}$ equal to zero.

In practice, the vibrational responses may be corrupted by noise, and thus Eq. (7) can simply be transformed into a constrained minimization problem.

$$\underset{\boldsymbol{f}}{\text{minimize}}\{\|\boldsymbol{f}\|_0 : \|\boldsymbol{y} - \boldsymbol{H}\boldsymbol{f}\|_2 \le \delta\} \tag{8}$$

where the bound δ is the tolerance of measurement error. Furthermore, the constrained minimization problem is frequently recast into an unconstrained form with l_0-norm penalty.

$$\underset{\boldsymbol{f}}{\text{minimize}}\{\|\boldsymbol{H}\boldsymbol{f} - \boldsymbol{y}\|_2^2 + \lambda\|\boldsymbol{f}\|_0\} \tag{9}$$

The residual term $\|\boldsymbol{H}\boldsymbol{f} - \boldsymbol{y}\|_2^2$ can reduce the influence of the noise included in measurements. The regularized term $\lambda\|\boldsymbol{f}\|_0$ taken as a penalty incorporates the sparsity prior of the impact forces in temporal and spatial domains. However, l_0-norm minimization Eq. (7) or regularization Eq. (9) is a typical NP-hard problem, which is not easy to be solved for highly under-determined inverse problems (Donoho 2006).

To circumvent this problem, one alternative convex relaxation is to replace the l_0-norm penalty with the l_1-norm penalty.

$$\underset{\boldsymbol{f}}{\text{minimize}}\{\|\boldsymbol{H}\boldsymbol{f} - \boldsymbol{y}\|_2^2 + \lambda\|\boldsymbol{f}\|_1\} \tag{10}$$

where $\|\boldsymbol{f}\|_1 = \sum_{i=1}^{n}|f_i|$ is the convex envelop of $\|\boldsymbol{f}\|_0$over the interval $\{\boldsymbol{f}: \|\boldsymbol{f}\|_\infty \le 1\}$. Notably, different from l_0-norm regularization in Eq. (10), l_1-norm regularization (as named Lasso regularization) in Eq. (10) is an equivalent convex optimization problem and it can be solved by many efficient algorithms such as gradient projection, iterative shrinkage-thresholding and interior point method that guarantee a globally optimal solution (Koh *et al*. 2007). The cost is that more measurements are required for sparse signal recovery (Chartrand and Staneva 2008, Liu *et al*. 2022). Donoho (2006) proved that under some conditions, for most large underdetermined systems, l_1-norm minimization can also generate the sparsest solution from a small number of measurements as l_0-norm minimization.

In this work, l_1-norm regularization is called the standard sparse regularization model for impact force identification. The l_1-norm penalty encourages small components in the impact force vector $\boldsymbol{f}$ to become zeros, preserves the local information with large magnitude, and thus yields a sparse solution. It is interesting to note that the solution of l_1-norm regularization often shows less sparsity than that of l_0-norm regularization. Larger elements in desired forces are penalized more heavily by the l_1-norm, while the penalizations of the l_0-norm on forces with different magnitudes are equal. Hence, l_1-norm regularization does not always yield a sufficiently sparse solution (see Fig. 1) (Qiao *et al*. 2019). In this context, the standard l_1-norm regularization for impact force identification tends to produce the underestimated solution.

Recently, it has been demonstrated that the nonconvex l_p ($0 < p < 1$) quasi-norm regularization bridging l_0-norm regularization and l_1-norm regularization can produce more accurate reconstruction with fewer measurements when compared to the convex l_1-norm regularization. In the present study, considering the desired sparse structure of impact force, we are interested in addressing the more challenging case of l_p-norm ($0 < p < 1$) regularization for the under-determined problem of impact force identification. The general framework of l_p-norm regularization is summarized as

$$\underset{\boldsymbol{f}}{\text{minimize}}\{\|\boldsymbol{H}\boldsymbol{f} - \boldsymbol{y}\|_2^2 + \lambda\|\boldsymbol{f}\|_p^p\} \tag{11}$$

where p is a tuning parameter. l_p-norm $\|\boldsymbol{f}\|_p$ is taken as the norm of the solution of impact force identification model. Such a problem is said to be convex when $p \geq 1$. Otherwise, it is nonconvex when $0 < p < 1$. The l_p-norm of a vector is defined for $0 < p \leq 1$.

$$\|\boldsymbol{f}\|_p = \left(\sum_{i=1}^{n} |f_i|^p\right)^{\frac{1}{p}} \tag{12}$$

The penalty $\|\boldsymbol{f}\|_p^p$ properly reflects different priors on the unknown force. It is intuitive that when $p \to 0$, the solution to Eq. (11) will be close to that of Eq. (9), thus achieving a sparser solution than solving Eq. (10). Theoretical investigations supported that for an under-determined system, the solution of l_p-norm minimization is also the sparsest one under some conditions (Lai and Wang 2011). Coping with different penalties often demands different regularization algorithms. Compared with l_1-norm regularization, a major problem of l_p-norm regularization is that Eq. (11) is a nonconvex, nonsmooth and non-Lipschitz optimization problem. Though solving Eq. (11) is more difficult than solving Eq. (10), many algorithms can still be applied to seek a local minimizer.

l_p-norm (0 < p < 1) minimization for solving an under-determined system requires weaker conditions to guarantee a successful recovery than the case $p = 1$. Theoretical results and numerical experiments have demonstrated that, compared to l_1-norm regularization, l_p-norm regularization ($0 < p < 1$) requires fewer measurements for exact signal reconstruction (Lai and Wang 2011).

Almost all the existing regularization methods for force identification can be considered as a special form of this regularization framework. When $p = 0$, the procedure counts the number of nonzero entries, which is referred to as l_0-norm regularization. When $p = 1$, it is l_1-norm regularization, which is called the standard sparse regularization in this paper. For l_p-norm ($p > 1$) regularization, researchers mainly focus on l_2-norm regularization, also called Tikhonov regularization, but its solution is non-sparse. l_0-norm regularization is an ideal method for impact force identification and would yield the sparsest solution but of little practical use, since its solution requires an intractable combinatorial search. l_1-norm regularization provides an alternative for sparse identification of impact force, which just needs to solve a quadratic programming problem but is less sparser than l_0-norm regularization.

To choose the proper penalty for impact force identification, the mismatch between the l_0-norm and the l_1-norm regularizations that we are trying to compensate using l_p-norm regularization with $0 < p < 1$, can be seen clearly in Fig. 1, where larger values are penalized more heavily by l_1-norm penalty than small ones. The limit case for $p = 0$ by penalizing all the nonzero values equally can be seen as more impartial than any other norms. If a very small value would be weighted as much as a large value, the minimization process will try to eliminate the smaller ones and enhance the larger ones. Due to the NP-hardness of l_0-norm penalty, it seems that there no hope of approximating $\|\boldsymbol{f}\|_0$ to any level of accuracy by a convex function. On the contrary, there exist various concave functions that can approximate $\|\boldsymbol{f}\|_0$. It is well-known that l_1-norm is the convex envelope of $\|\boldsymbol{f}\|_p^p$ over the region [-1, 1]. When $0 < p < 1$, non-zero components are penalized increasingly for decreasing values of p; the smaller p is, the larger is the penalty on small values of solutions **f** (e.g., near zeros); conversely, for large values (e.g., the peak amplitudes), the smaller p is, the smaller is the penalty on these values. This implies that Eq. (11) imposes a relatively large penalty on small nonzero components, encouraging them to become zero, while larger values are more heavily penalized by l_1-norm regularization. Therefore, for impact force identification, l_p-norm regularization can yield a sparser solution and has the potential to compensate for the underestimation that occurs with l_1-norm regularization.

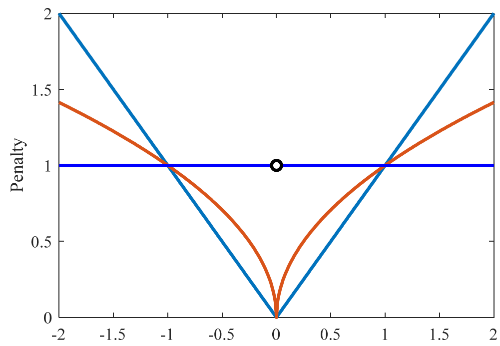

Fig. 1 l_p-norm penalty functions $\|\boldsymbol{f}\|_p^p$ for $p = 1$, $p = 1/2$ and $p = 0$

4. Iteratively reweighted l_1-norm minimization algorithm

Finding a minimizer of l_p-norm ($0 \leq p < 1$) model remains a big challenge, due to its nonconvex nature. It raises the question whether one can find another alternative which not only finds a more accurate solution than l_1-norm regularization but also is easier to be solved than l_0-norm regularization. In this section, we present a simple iteration procedure to solve the under-determined l_p-norm regularization model of impact force identification, which aims to find a sparse and accurate solution of Eq. (11). Indeed, it has been shown that l_p-norm can be approximated by a series of weighted l_1-norm, where the existing Lasso algorithms can be efficiently applied (Wipf and Nagarajan 2010). Candes *et al.* (2008) proposed an iteratively reweighted l_1-norm minimization algorithm (IRL1) corresponding to the $p = 0$ case for improving the sparsity and accuracy of l_1-norm minimization. Extensive numerical experiments indicate that IRL1 does outperform l_1-norm minimization in many situations (Candes *et al.* 2008, Wipf and Nagarajan 2010).

The core idea of IRL1 is to replace the l_p-norm penalty by an equivalent iterative procedure based on a weighted l_1-norm penalty. Using l_1-norm penalty to majorize nonconvex l_p-norm penalty, the resulting algorithm can be interpreted as a sequence of weighted l_1-norm minimization problems, in which each set of weights depends on the previous iteration. IRL1 is generally used for constrained l_p-norm minimization problems in a noise-free case.

$$\underset{f}{\text{minimize}}\{\|\boldsymbol{f}\|_p^p, \boldsymbol{y}=\boldsymbol{Hf}\}, 0<p<1 \tag{13}$$

Here, to handle the measurement noise in impact force identification, IRL1 is extended to the unconstrained l_p-norm regularization problem.

$$\underset{f}{\text{minimize}}\{\|\boldsymbol{Hf}-\boldsymbol{y}\|_2^2+\lambda\|\boldsymbol{f}\|_p^p\}, 0<p<1 \tag{14}$$

The model in Eq. (14) is also called the denoising model of Eq. (13). IRL1 consists in constructing a sequence $\{\boldsymbol{f}^{(k)}\}$ recursively by defining $\boldsymbol{f}^{(k+1)}$ as a solution of the following weighted l_1-norm regularization model.

$$\boldsymbol{f}^{(k+1)} \in \underset{f}{argmin}\left\{\|\boldsymbol{y}-\boldsymbol{Hf}\|_2^2+\lambda\left\|\boldsymbol{W}^{(k+1)}\boldsymbol{f}\right\|_1\right\} \tag{15}$$

where k is the iteration and the weight matrix is $\boldsymbol{W}^{(k+1)}=\text{diag}[\omega_1^{(k+1)},\omega_2^{(k+1)},\ldots,\omega_n^{(k+1)}]$. IRL1 solves a series of l_1-norm regularization problems to approximate the optimal solution of l_p-norm regularization. To improve the sparsity of the solution, the weights can be chosen as inversely proportional to the magnitudes of the components of the true solution. Typically, the optimal weight matrix $\boldsymbol{W}$ is not known exactly. Because the true impact force $\boldsymbol{f}$ is unknown, it is suggested that $\boldsymbol{W}$ is determined according to the current iteration and updated after each iteration.

$$\omega_i^{(k+1)}=\frac{1}{\left(\left|f_i^{(k)}\right|+\eta\right)^{1-p}}, i=1,\ldots,n \tag{16}$$

where $0<\eta\ll 1$ is a given small parameter to avoid division by zeros. The solution of Eq. (14) is set to be $\boldsymbol{f}^{(k+1)}$, based on which the new weight matrix $\boldsymbol{W}^{(k+1)}$ is computed by Eq. (16).

Large weights discourage nonzero elements in identified impact force. On the contrary, small weights encourage nonzero elements. Naturally, for a small $\left|f_i^{(k)}\right|\to 0$, there is a large weight value $\omega_i^{(k+1)}$ in Eq. (16) when p is fixed. Furthermore, as $p\to 0$, the weight value $\omega_i^{(k+1)}$ becomes large, when $\left|f_i^{(k)}\right|$ is small enough. Conversely, as $p\to 0$, the weight value $\omega_i^{(k+1)}$ becomes small, when $\left|f_i^{(k)}\right|$ is large enough (i.e., the impulse force). IRL1 attempts to find a local minimum of a nonconvex l_p-norm regularization model for impact force identification. It has been proved that under some conditions, the solutions of IRL1 can converge to a stationary point of l_p-norm regularization that is an approximation of l_0-norm regularization (Lai and Wang 2011). Although no analytic solution exists, many existing convex algorithms (e.g., interior point method) can be adopted to solve Eq. (15).

Therefore, the primary idea of IRL1 is to define a weight based on the current iterate, solve the weighted l_1-norm regularization, and thus use its solution to define a new weight. The pseudo code of IRL1 for the unconstrained regularization model of the impact force inverse problem is summarized as **Algorithm 1**. It is necessary to point out that l_p-norm regularization together with IRL1 allows arbitrary choices for $0\le p\le 1$. The reweighted l_1-norm minimization developed for enhanced sparse regularization of impact force identification, is the special instance of the algorithm with $p=0$ (Qiao *et al*. 2019).

Algorithm 1: Iteratively reweighted l_1-norm minimization algorithm for solving unconstrained l_p-norm regularization problem of impact force identification

Input: Transfer function matrix $\boldsymbol{H}\in\mathbb{R}^{nM\times nN}$, measured response $\boldsymbol{y}\in\mathbb{R}^{nM\times 1}$, regularization parameter λ and stability parameter η, the norm $p\in[0,1]$.

Step 1: Initialize the iteration count k=0, and the weight matrix to be the identity matrix, i.e., $\boldsymbol{W}^{(0)}=\boldsymbol{I}$.

Step 2: Solve the weighted l_1-norm regularization problem, i.e., Eq. (15).

Step 3: Update the weights ω_i, using Eq. (16).

Step 4: Terminate on convergence or when k attains a specified maximum number of iterations k_{max}. Otherwise, let $k=k+1$ and go to Step 2.

Output: Identified impact force $\boldsymbol{f}$ consisting of the impact location and the force time-history.

In Step 1, it is important to determine the initialization $\boldsymbol{f}^{(0)}$ for the successful impact force identification. It is assumed that the iterations begin with a vector (e.g., the l_1-norm solution) sufficiently close to the desired solution. The weighted l_1-norm regularization is initialized in the first iteration ($k=0$), where the starting weight matrix $\boldsymbol{W}^{(0)}$ is set to be an identity one. It implies that Step 2 is actually to solve a standard l_1-norm regularization problem, i.e., Eq. (10). It means that the solution of the standard l_1-norm regularization that was developed for impact force identification (Qiao *et al*. 2017), is selected as a reasonable initialization of l_p-norm regularization with $0\le p<1$.

Step 2 corresponds to solving a weighted l_1-norm regularization problem. The scheme is easy to implement, since each step reduces to a standard l_1-norm regularization model. In order to implement each reweighted algorithm using the existing convex solver, we make straightforward modification of the optimization problem Eq. (15). An intermediate variable $\boldsymbol{x}$ is defined as

$$\boldsymbol{x}=\boldsymbol{W}^{(k)}\boldsymbol{f} \tag{17}$$

Since the weight matrix is a diagonal one, the unknown impact force is expressed as

$$\boldsymbol{f}=\left(\boldsymbol{W}^{(k)}\right)^{-1}\boldsymbol{x} \tag{18}$$

Substituting Eqs. (17) and (18) into Eq. (15), an equivalent optimization problem can be obtained

$$\boldsymbol{x}^{(k)} = \underset{\boldsymbol{x}}{argmin}\left\{\left\|\boldsymbol{y} - \boldsymbol{H}\left(\boldsymbol{W}^{(k)}\right)^{-1}\boldsymbol{x}\right\|_2^2 + \lambda\|\boldsymbol{x}\|_1\right\} \quad (19)$$

Setting $\boldsymbol{A} = \boldsymbol{H}\left(\boldsymbol{W}^{(k)}\right)^{-1}$, the standard l_1-norm regularization model is derived as

$$\boldsymbol{x}^{(k)} = \underset{\boldsymbol{x}}{argmin}\{\|\boldsymbol{y} - \boldsymbol{A}\boldsymbol{x}\|_2^2 + \lambda\|\boldsymbol{x}\|_1\} \quad (20)$$

It relaxes the original l_p-norm regularization problem to a sequence of l_1-norm problems. For each p, IRL1 solves a series of l_1-norm regularization to approximate the original nonconvex optimization problem. Each iteration of IRL1 simply requires solving one l_1-norm regularization problem, which can be implemented readily by using many efficient algorithms such as interior point method. Here, a robust solver, the primal-dual interior point method (PDIPM), is suggested to solve the l_1-norm regularization problem of impact force identification. PDIPM has been successfully applied for solving the standard l_1-norm regularization model of impact force identification in authors' previous work (Qiao *et al.* 2017, 2019). It is known that the reconstruction accuracy of the solution of a regularization problem depends seriously on the regularization parameter λ. However, the selection of proper regularization parameters is often hard. According to the previous work (Qiao *et al.* 2017), the regularization parameter is empirically set $\lambda = 0.01\|2\boldsymbol{H}^T\boldsymbol{y}\|_\infty$.

In Step 3, the weight matrix $\boldsymbol{W}$ is adaptively updated according to the current solution, and the updated weight matrix after each iteration is used to obtain the next solution $\boldsymbol{f}^{(k+1)}$. Each weight $\omega_i^{(k+1)}$ is only a function of the preceding iterative solution $f_i^{(k)}$. In order to implement Step 3, a stability parameter η is introduced to ensure the stability when small components in the previous solution $\boldsymbol{f}^{(k)}$ go to zero. According to the work (Qiao *et al.* 2019), the value of η should be set much smaller than the expected nonzero magnitudes. The identification of impact force is reasonably robust with respect to the choice of η. The stability parameter can be set $\eta = 0.00001$. Such an iterative algorithm for updating the weights ω_i allows for successively better estimation of the nonzero supports, i.e., the pulse interval of impact force.

In Step 4, the stopping condition can be chosen as either a maximal number of iterations or as a convergence criterion. It should be noted that as for any nonconvex optimization problem, there is no way to derive any guarantees regarding the convergence. Nevertheless, IRL1 empirically works well for l_p-norm regularization and is easily implemented. Numerical experiments (Foucart and Lai 2009) demonstrated that the iteration converges to the sparsest solution with an overwhelming probability. When an initial point is properly chosen, the convergence of the enhanced sparse regularization using IRL1 has been empirically demonstrated in numerical and experimental examples (Candes *et al.* 2008, Qiao *et al.* 2019). Actually, few reweighting iterations or even a single iteration of IRL1 are sufficient to address the impact force identification problem, the solutions of which can be sparser and more accurate than those of the standard l_1-norm regularization. For all under-determined tested cases in this paper, each reweighted algorithm is executed by only five iterations. Clearly, the main computational cost in **Algorithm 1** is consuming on solving a series of l_1-norm regularization problems. Much of the benefit of solving l_p-norm regularization comes from first few reweighting iterations, and the additional computational cost is quite moderate, compared to l_1-norm regularization. The required reconstruction time is generally more than with $p = 1$ but much less than with $p = 0$.

5. Numerical examples using a simply supported plate

In this section, we start with numerical examples conducted on a simply supported plate to confirm the effectiveness and applicability of the proposed l_p-norm ($0 \leq p < 1$) regularization method in improving the reconstruction accuracy of impact force as well as the impact localization from highly incomplete measurements under different noise levels, compared to the standard l_1-norm regularization. Single-source and double-source impact forces acting on nine potential locations the sparsity of which are different, will be localized and reconstructed by using only a single acceleration response.

Under impact circumstances, the peak force amplitude of impact events matters much for the assessment of the structural integrity (Qiu and Yuan 2011). Hence, the peak relative error (PRE) between the exact and identified solutions is calculated to quantify the performance of regularization methods in solving the ill-posed inverse problem of impact force identification.

$$\text{PRE} = \frac{max(\boldsymbol{f}_{\text{exact}}) - max(\boldsymbol{f}_{\text{identified}})}{max(\boldsymbol{f}_{\text{exact}})} \times 100\% \quad (21)$$

where $max(\boldsymbol{f})$ denotes the maximum amplitude of impact force; $\boldsymbol{f}_{\text{exact}}$ and $\boldsymbol{f}_{\text{identified}}$ is the exact and identified impact forces, respectively.

5.1 Problem description

The distribution of impact locations and measurement locations over the simply supported plate is limned in Fig. 2. The detailed parameters of the plate can be found (Qiao *et al.* 2016b). Although the exact location of the impact event is unknown, nine possible impact locations uniformly distributed over the surface of the plate are considered in impact force identification. To take advantage of the spatial distribution of impact locations, it is supposed that one or two of nine different locations of the plate are excited. The single-source impact force acting on location 6# (300 mm, 375 mm) is defined as

$$f_0(t) = F_0 e^{(-2\pi f_0 (t-t_0)^2)} \quad (22)$$

The double-source impact forces applied at location 3# (150 mm, 375 mm) and location 6# (300 mm, 375 mm) are respectively defined as

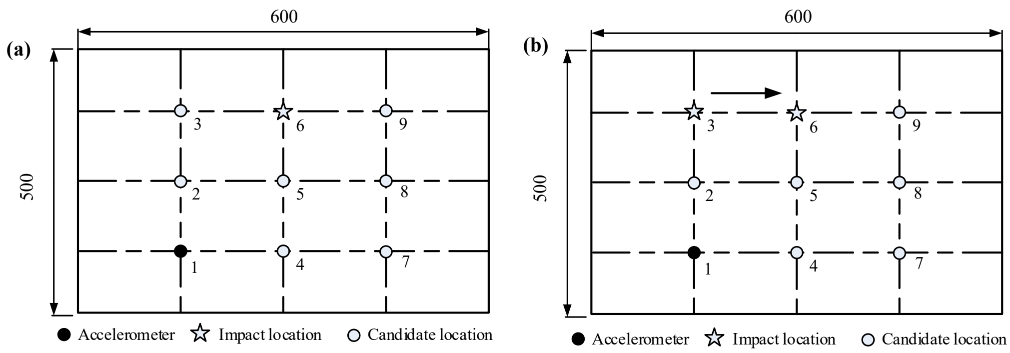

Fig. 2 The distribution of impact forces and measurement locations of the simply supported plate: (a) the single-source impact-force case; and (b) the double-source impact-force case (dimensions in mm)

$$f_1(t) = F_1 e^{(-2\pi f_0 (t-t_1)^2)}; f_2(t) = F_2 e^{(-2\pi f_0 (t-t_2)^2)} \quad (23)$$

where the center frequency f_0 is used to adjust the frequency band of interest. When $f_0 = 120000$ Hz, the simulated impact force with a short duration has a good agreement with the actual one in Section 6. For the single-source case, the peak force $F_0 = 120\,N$ is obtained at $t_0 = 0.1948\,s$; for the double-source case, the first impact force acts on point 3# whose peak force $F_1 = 120\,N$ is obtained at $t_1 = 0.1948\,s$ and the second one acts on point 6# whose peak force $F_2 = 100\,N$ is obtained at $t_2 = 0.5854\,s$. A total simulated duration of 1s is considered, assuming the sampling frequency of 2048 Hz. The impact force is not assumed to be concentrated at a point. Hence, this work involves identifying multiple impact forces rather than a single concentrated force.

Given the impact force and the transfer function matrix, the transient acceleration response of location 1# (150 mm, 125 mm) used for impact force identification is generated from a forward computation. In order to evaluate the effect of measurement noise on the identified impact force using l_p-norm regularization, the simulated noise is added to the exact acceleration $\boldsymbol{y}$.

$$\tilde{\boldsymbol{y}} = \boldsymbol{y} + \boldsymbol{e} = \boldsymbol{y} + l_{\text{noise}} \cdot \text{std}(\mathbf{y}) \cdot (2 \cdot \text{rand}(n,\ 1) - 1) \quad (24)$$

where $\tilde{\boldsymbol{y}}$ represents the polluted response; $\mathbf{e}$ denotes the additive noise; l_{noise} indicates the noise level; the MATLAB script function $\text{std}(\mathbf{y})$ denotes the standard deviation of $\mathbf{y}$; the MATLAB script function $\text{rand}(n, 1)$ denotes an $n \times 1$ random vector satisfying the uniform distribution on the interval (0, 1). Here, four simulations with the noise levels l_{noise} = 10%, 40%, 60% and 100% are considered. The simulated noise will inversely propagate into the identified impact forces.

In this work, only a single acceleration response point 1# is utilized for identifying the impact location and the force history, such that the number of potential impact locations (nine locations) greatly exceeds the number of measurements (one sensor). The impact location and the force history forces can be simultaneously computed by l_p-norm ($0 \le p \le 1$) regularization from highly imperfect and incomplete data. The dimension of the excitations $\boldsymbol{f}$ composed of nine assumed impact force vectors $\boldsymbol{f}_j \in R^{2048\times1}$ is 18432×1; the dimension of the transfer function matrix $\boldsymbol{H}$ in Eq. (5) composed of nine transfer matrices $\boldsymbol{H}_{1j} \in R^{2048\times2048}$ (j = 1,…,9) is 2048×18432; the dimension of the measurement vector $\boldsymbol{y}$ is only 2048×1. Hence, such a problem of impact force identification is highly under-determined. All simulated cases are successively done for each $p \in \{0, 0.1, 0.2, \ldots, 0.9, 1\}$. Let us point out that when p = 1, it corresponds to the standard l_1-norm regularization (Qiao *et al.* 2017). When p = 0, the l_p-norm regularization model using IRL1 as a special case corresponds to the enhanced sparse regularization method Qiao *et al.* 2019). In each case, the peak relative error and the number of non-zero components in identified impact forces are computed.

5.2 Single-source impact force identification

It starts with the identification of the single-source impact force using l_p-norm regularization from heavily contaminated and highly incomplete response. We first fix p = 1/2 and test l_p-norm regularization in determining the impact location and simultaneously reconstructing the force time-history under four noise levels. To see the possible impact force at each point and then localize the impact force, the identified impact force signal $\boldsymbol{f} \in \boldsymbol{R}^{18432\times1}$ is divided into nine vectors, as illustrated in Fig. 3. For each case, the exact impact force is also given (Location = 0). It is remarkable that under four noise levels, the impact force is successfully localized from nine candidate locations using only a single acceleration response. The location 6# that coincides with the actual force location, is the only one which is clearly excited. Fig. 3 depicts that the nonzero entries of the $l_{1/2}$-norm solutions strongly concentrate on the peak profile of impact force. The $l_{1/2}$-norm solutions are sufficiently sparse and match the exact one quite well. The reconstructed force histories of other locations are much smaller and have no clear impulsive feature. Hence, it helps improve the impact localization and determine the occurrence time of impact force. As the noise level increases, there exist more random spurious values that are irrelevant to the true impact force.

Subsequently, l_p-norm ($0 \le p < 1$) regularization together with l_1-norm regularization is applied to identifying the single-source impact force from a single acceleration response. As shown above, l_p-norm regularization works

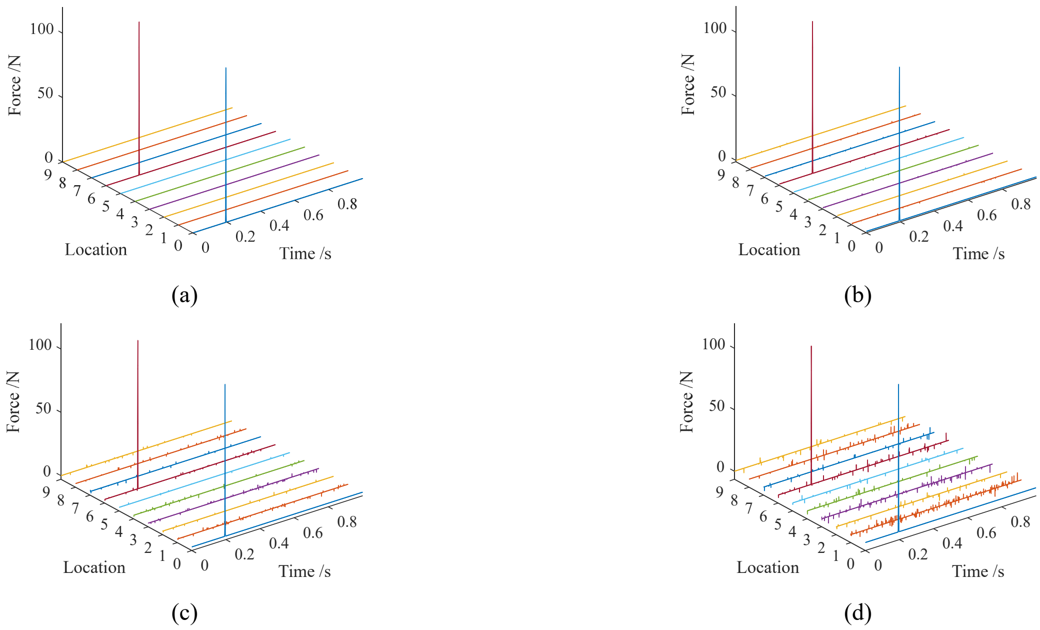

Fig. 3 $l_{1/2}$-norm regularization for identifying the single-source impact force acting on location 6# under different noise levels: (a) 10%; (b) 40%; (c) 60%; and (d) 100%

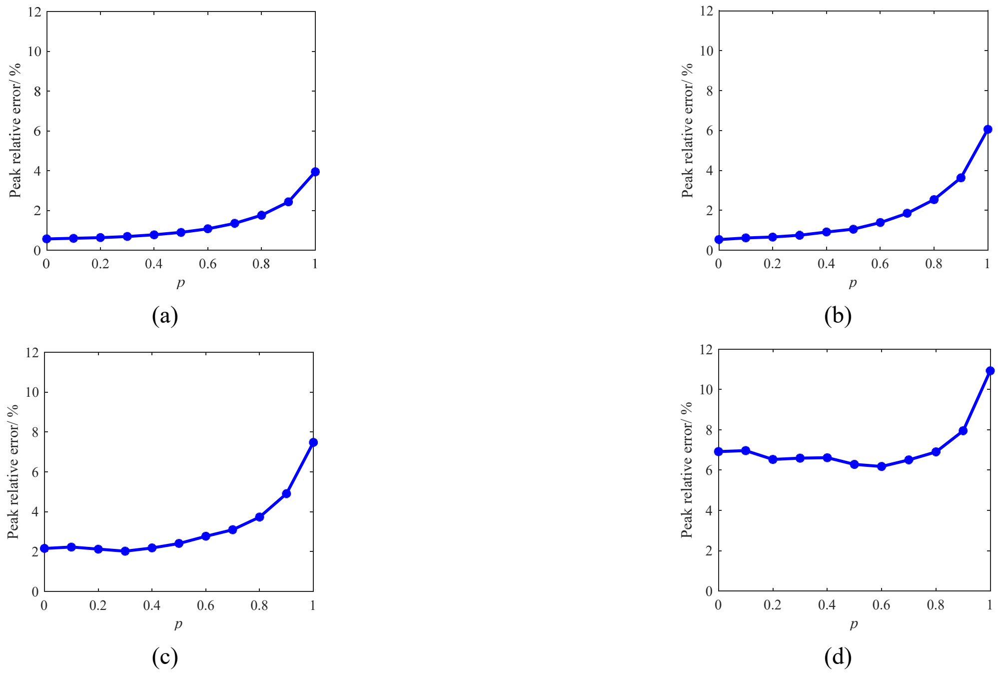

Fig. 4 The peak relative error of the identified single impact force acting on location 6# using l_p-norm regularization as a function of p under different noise levels: (a) 10%; (b) 40%; (c) 60%; and (d) 100%

well in identifying the impact location. The peak value of impact force is an important indicator in structural health monitoring. Here, we focus on the identification of the maximum value of impact force, compared to the standard l_1-norm regularization. Fig. 4 depicts the peak relative error between the exact and identified impact forces using l_p-norm regularization as a function of p ($0 \le p \le 1$) under four noise levels. Differences of l_p-norm regularization with $0 \le p < 1$ for improving the peak force amplitude are quantitatively compared. It can be seen from Fig. 4 that the l_1-norm solutions are underestimated, meaning the peak of the identified force is lower than the exact solution, particularly when $l_{noise} = 100\%$ (see Fig. 4(d)). A significant improvement in identifying the peak force amplitude is observed using l_p-norm ($0 \le p < 1$) compared to l_1-norm regularization across all four noise cases. Even for $p = 0.9$, there is a noticeable improvement over l_1-norm regularization. The peak relative errors of l_p-norm solutions ($0 \le p \le 1/2$) are nearly half of those of l_1-norm solutions. In the same condition, as the noise level increases, the peak

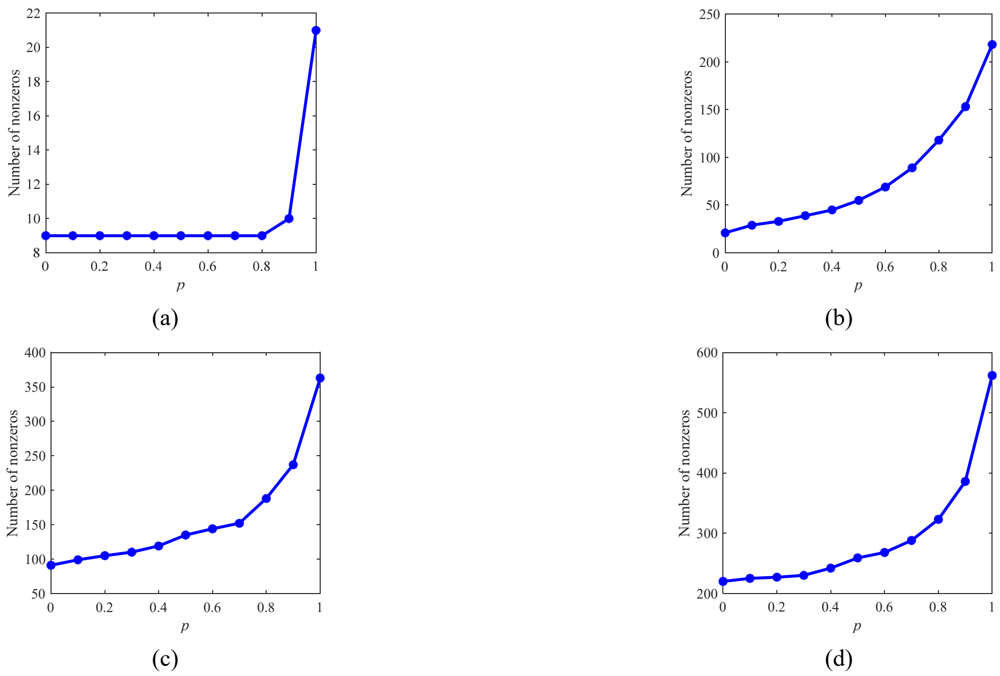

Fig. 5 Number of nonzero components in the identified single impact force acting on location 6# using l_p-norm regularization as a function of p under different noise levels: (a) 10%; (b) 40%; (c) 60%; and (d) 100%

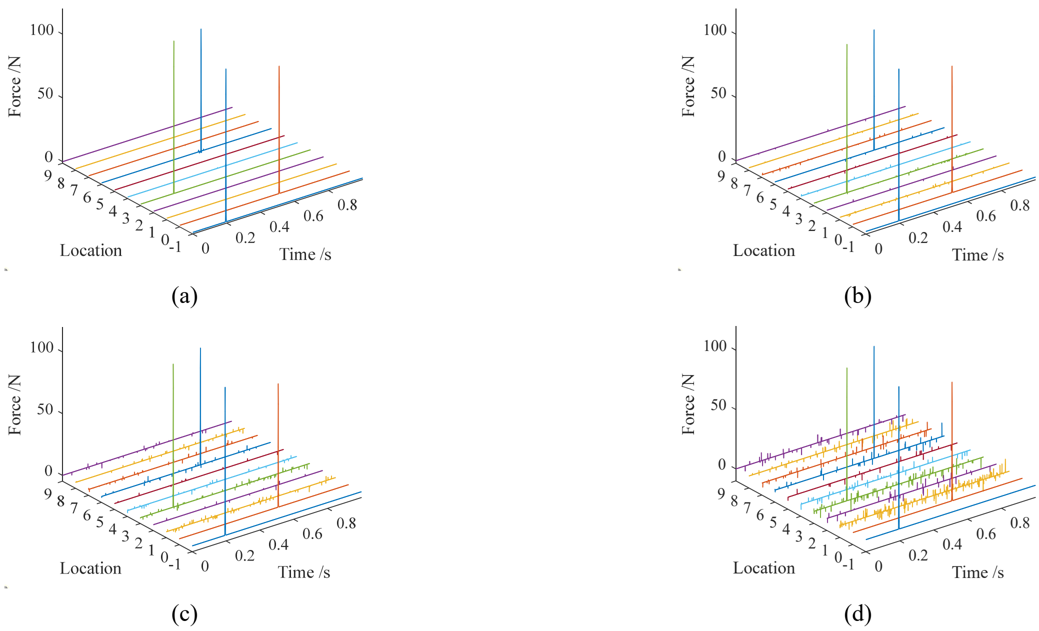

Fig. 6 $l_{1/2}$-norm regularization for identifying the double-source impact forces acting on locations 3# and 6# under different noise levels: (a) 10%; (b) 40%; (c) 60%; and (d) 100%

relative error of l_p-norm ($0 \leq p < 1$) solutions also increases. One can see from Fig. 4 that the peak relative error has a monotonous reduction tendency as $p \rightarrow 0$, when the noise levels are small (e.g., l_{noise} = 10% and l_{noise} = 40%). It suggests that decreasing p improves the robustness of l_p-norm regularization to noise. It coincides with the intuition that the performance of l_p-norm regularization is improved when p decreases. The change of the peak relative error is large for $1/2 \leq p \leq 1$; but the change is small for $0 \leq p \leq 1/2$. The enhanced sparse regularization (p = 0) cannot always yield the most accurate solution, particularly when the noise levels are large (e.g., l_{noise} = 60% and l_{noise} = 100%). For example, when l_{noise}= 100%, the peak relative error of $l_{0.6}$-norm is smallest. It is not necessary to make p much smaller for further improving the identification accuracy. The similar results have been observed in Xu'work on $l_{1/2}$-norm regularization (Xu *et al* 2012).

We compare the sparsity of l_p-norm regularization with l_1-norm regularization in solving the under-determined inverse problem of impact force identification. Fig. 5 lists the number of nonzero elements in identified single impact force as a function of p under four noise levels. It is clear that l_p-norm regularization generates sparser solutions than l_1-norm regularization. One can see from Fig. 5 that l_p-norm regularization with $0 \leq p \leq 0.8$ performs particularly well in finding the sparse solution of impact force identification, when l_{noise} =10%. The sparsity significantly increases as p decreases, when the noise levels are high. As the noise level increases, the sparsity of the solution declines. We see a greater improvement for the smaller p corresponding to a sparser solution (see Fig. 5), with the reduction in peak relative error up to 50% or more (see Fig. 4). Therefore, although a single acceleration response is inversely used, l_p-norm regularization for impact force identification with IRL1 still ensures the sparsity and accuracy of the solution.

5.3 Double-source impact force identification

In the second one of under-determined force identification problems, the localization and reconstruction of the double-source impact forces acting on nine possible locations are implemented by l_p-norm regularization under four noise levels. The under-determined system in Eq. (6) has the same dimension as the case in Section 5.2. The difference lies in the sparsity of the solution. Here the force vector **f** includes two impulsive forces. The following examples are conducted to show the feasibility of l_p-norm regularization, when the sparsity decreases. shows that two identified impact forces using $l_{1/2}$-norm regularization are well localized on locations 3# and 6# under four noise levels. The values in other assumed locations are quite small and ignored, leading to an accurate localization of the impact force. The two exact impact forces are also shown in, corresponding to Location = -1 and Location= 0. The histories of $l_{1/2}$-norm solutions match the exact ones pretty well. The case of l_{noise} = 100% in responses is taken as example. The peak value for the first identified impact force is 111.9 N, while the reference value is 120 N, yielding a peak relative error of 6.75%. The peak value for the identified second impact force is 94.38 N, with a reference value of 100 N, yielding a peak relative error of 5.62%.

As we can see from Fig. 7, l_p-norm regularization with $0 \leq p < 1$ does have much more identification accuracy than l_1-norm regularization. The first impact is the one acting on locations 3# and the second impact is the one acting on locations 6#. When the noise level is low, e.g., l_{noise} = 10%, l_1-norm regularization can also achieve acceptable solutions, the peak relative error of which is less than 10%. When the noise level is high in Figs. 7(c) and (d), the peak amplitude of the identified impact force using l_1-norm regularization is dramatically underestimated. l_p-norm regularization is robust with respect to noisy measurements. When p increases from 0 to 1, the peak relative error increases nearly two times. All the peak relative errors of two identified impact forces using l_p-norm regularization are less than 10% under four noise levels. Consequently, the identified impact forces computed by l_p-norm regularization with $0 \leq p < 1$ are much improved. It is the intuition that decreasing p results in a more accurate solution, typically for l_{noise} = 40% in Fig. 7(b). However, it is not true for all cases in Fig. 7. Actually, the improvement of impact force identification using l_p-norm regularization has no significant differences for $0 \leq p < 1/2$. One case see from Figs. (c) and (d) that for $0.3 \leq p \leq 0.6$, the peak relative error of l_p-norm solutions is smallest. It appears that reducing p less than 1/2 gives only a slight decrease or even increase in peak relative error. Similar phenomenon has been discovered by Xu *et al.* (2012). Figs. 7(c) and (d) also reveal that the choice of $p = 0$

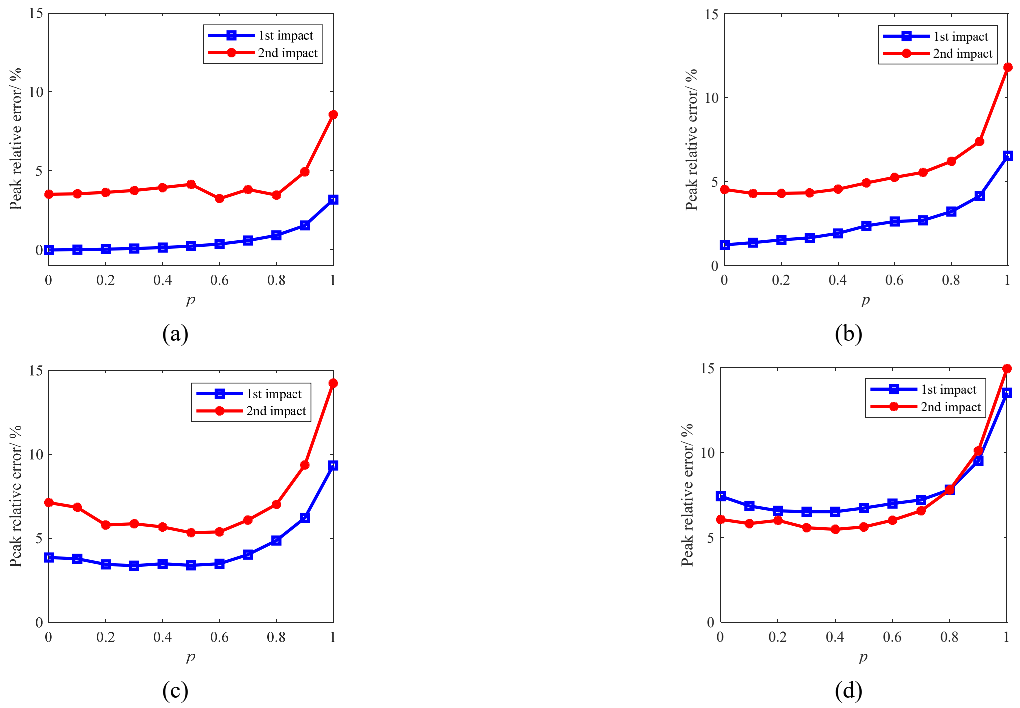

Fig. 7 The peak relative error of identified two impact forces acting on locations 3# and 6# using l_p-norm regularization as a function of p under different noise levels: (a) 10%; (b) 40%; (c) 60%; and (d) 100%

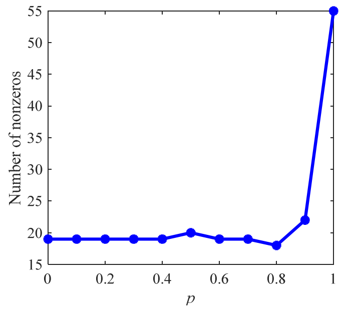

(a)

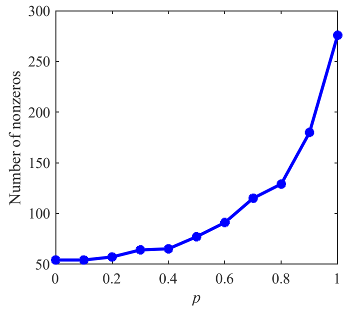

(b)

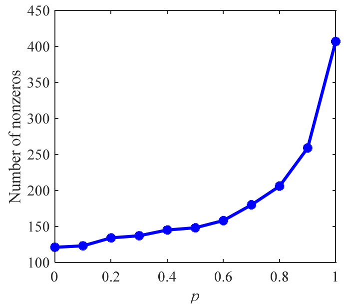

(c)

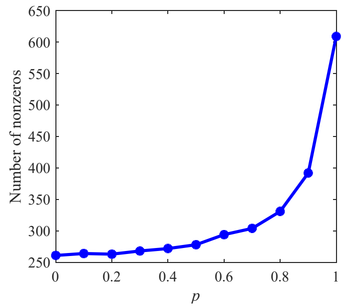

(d)

Fig. 8 The number of nonzero components in identified two impact forces acting on locations 3# and 6# using l_p-norm regularization as a function of p under different noise levels: (a) 10%; (b) 40%; (c) 60%; and (d) 100%

is not unequivocally the best choice for a single p in impact force identification. It should be noted that compared with the single-source impact force identification, the peak relative errors of the identified double-source impact forces are commonly large but acceptable under the same noise level. One reasonable explanation is that for the same dimension of the inverse problem, as the non-zeros of solutions increase, the reconstruction accuracy will reduce in sparse regularization.

Fig. 8 displays results where the number of nonzero elements in identified two impact forces using l_p-norm ($0 \leq p < 1$) regularization is drawn with p. It is noteworthy that the l_p-norm solutions are significantly sparser than the l_1-norm solutions, even in the presence of substantial noise. As the noise level increases, nonzero components in sparse solutions significantly increase. l_p-norm regularization with $0 \leq p \leq 0.8$ performs particularly well in finding the sparsest solutions of the inverse problem of impact force identification. The sparsity of l_p-norm regularization is helpful in localizing the impact force. It implies that the nonconvex l_p-norm regularization requires less measurements in solving the under-determined problem of impact force identification.

The numerical simulations demonstrate that, regardless of the value of $0 \leq p < 1$, l_p-norm regularization with IRL1 outperforms standard l_1-norm regularization for impact force identification in terms of both sparsity and accuracy, even when the responses are highly polluted and incomplete. One can see from Figs. 4-5 and Figs. 7-8 that when the number of the actual impact force increases, the sparsity and accuracy of the solution will decay.

6. Experimental validation using a cantilever plate

In this section, the proposed l_p-norm ($0 \leq p \leq 1$) regularization method for impact-force localization and reconstruction is validated using experimental data obtained from a cantilever plate. The influence of six measured locations of acceleration on the identification accuracy is analyzed. Single-source and double-source impact forces acting on nine possible locations are localized and reconstructed by using only a single accelerometer. The advantage of l_p-norm ($0 \leq p < 1$) regularization over l_1-norm regularization is demonstrated under different acceleration responses.

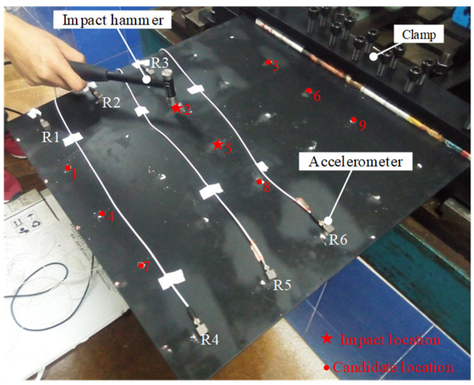

Fig. 9 The cantilever plate experimental set-up applied for impact force identification

6.1 Experiment description

The structure under study applied for impact force identification is a cantilever plate, set up as shown in Fig. 9. One plate edge is fully constrained by a clamp. The material is structural steel. The dimensions are 500 mm × 600 mm × 5 mm. As described in Section 5, the impact forces are assumed to act on spatially discrete nine locations. A PCB 086C01 impact hammer is used to exert the impact force vertically at one or two points of nine locations. But we do not know which one is chosen in the procedure of impact force identification. The integral force sensor inserted in the tip of the hammer is used to measure the input force as the reference. The top surface of the plate is instrumented with six PCB 333B32 accelerometers for measuring the vertical response, labeled as **R1**-**R6**. All the measured responses for impact force identification are away from the excitation locations. A preliminary impact test is conducted for determining the transfer function matrix **H** between six measured locations and nine candidate impact locations. The input force and the response synchronously recorded by a 16-channel LMS data acquisition system are sampled at

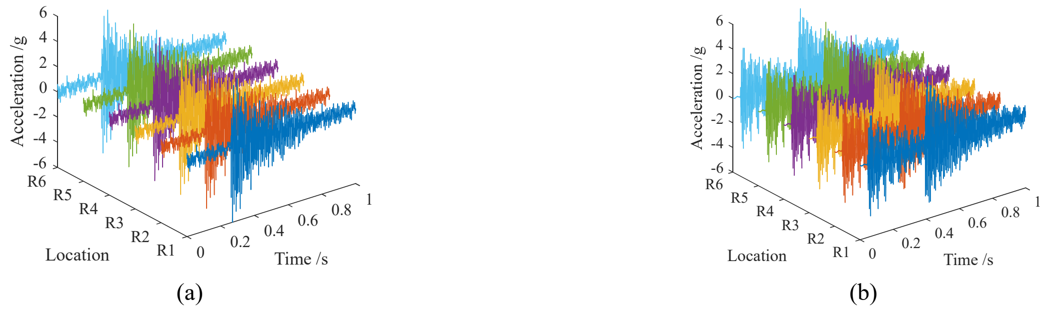

Fig. 10 The acceleration responses of six measured locations subjected to impact events: (a) the single-source impact force acting on location 2#; and (b) the double-source impact forces acting on locations 2# and 5#

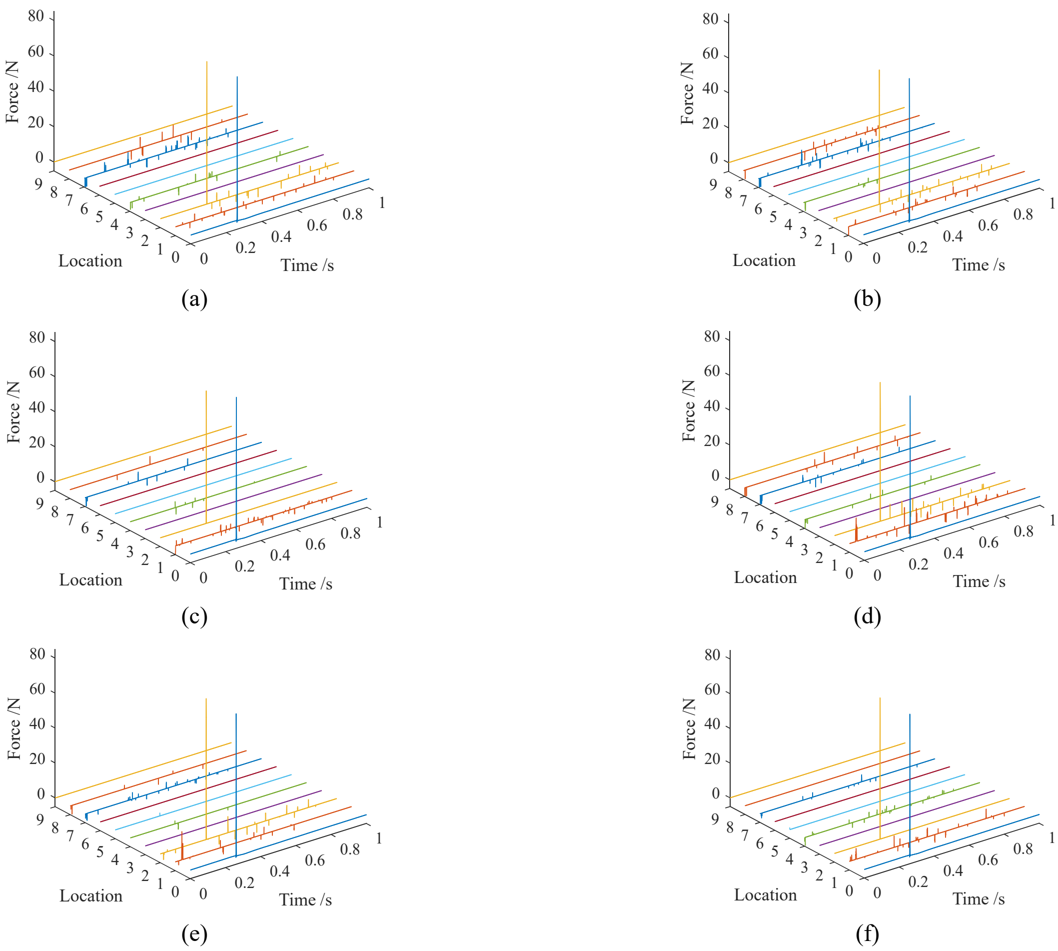

Fig. 11 $l_{1/2}$-norm regularization for identifying the single-source impact force acting on location 2# from six acceleration responses: (a) R1; (b) R2; (c) R3; (d) R4; (e) R5; and (f) R6

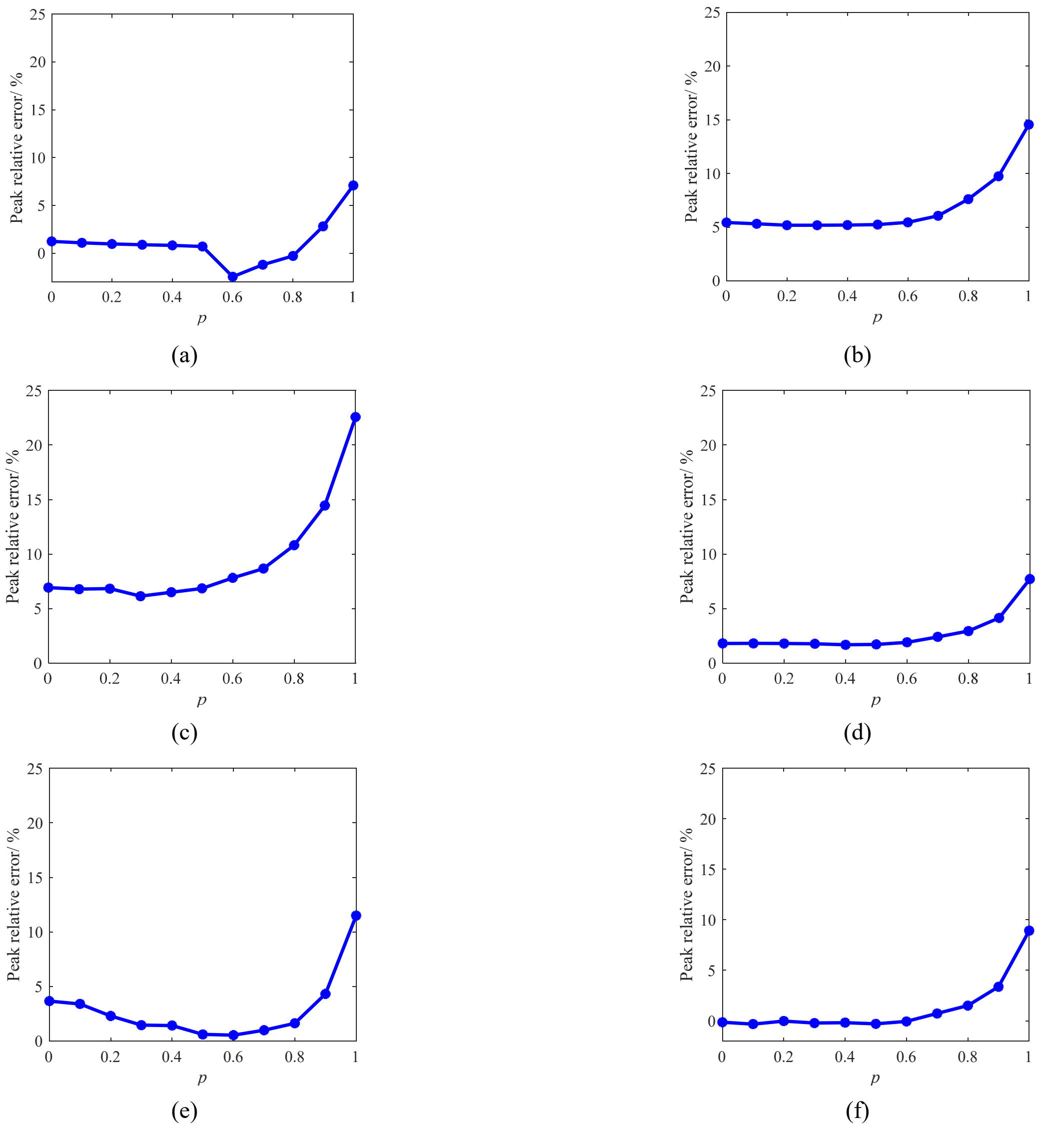

Fig. 12 The peak relative error of identified single impact force acting on location 2# using l_p-norm regularization as a function of p from six acceleration responses: (a) R1; (b) R2; (c) R3; (d) R4; (e) R5; and (f) R6

2048 Hz. The impact testing module of LMS data acquisition system is applied for obtaining frequency response functions. Through inverse fast Fourier transform of frequency response functions.

Successive impacts are applied by impact hammer at different locations (2# and 5#) on the plate. Fig. 10 illustrates six acceleration responses subjected to the single-source impact force acting on location 2# and the double-source impact forces acting on locations 2# and 5#. A total of 1 s data is truncated for impact force identification. The time response of each impact event displays a rapid attenuation phenomenon. The current impact response also contains the response of the previous impact force, as shown in Fig. 10(a). There exists overlap among the adjacent impact events, as shown in Fig. 10(b). The influence from the previous impact force is regarded as the measurement noise. l_p-norm ($0 \leq p \leq 1$) regularization is applied, and the impact locations are assumed to be from the nine points on the plate shown in Fig. 9.

6.2 Single-source impact force identification

A similar analysis process as Section 5.2 is conducted. Fig. 11 shows the reconstruction and localization results of the single-source impact force using $l_{1/2}$-norm (p = 1/2) regularization from six acceleration responses, in which the measured impact force as reference is also given. The impact force acting on location 2# is well localized no matter which one acceleration response is chosen for inverse analysis. It can be observed from Fig. 11 that all the $l_{1/2}$-norm solutions using six acceleration responses are sufficiently sparse, leading to a much better localization. Although there exist many spurious peaks in the time domain, it cannot result in unacceptable identified impact forces. Fig. 11 shows the time histories of the identified forces are in good overall agreement with the measured force. The disturbance from the previous impact response is greatly inhibited in the identified impact force. In detail, the peak value of the measured impact force is 81.21 N. The

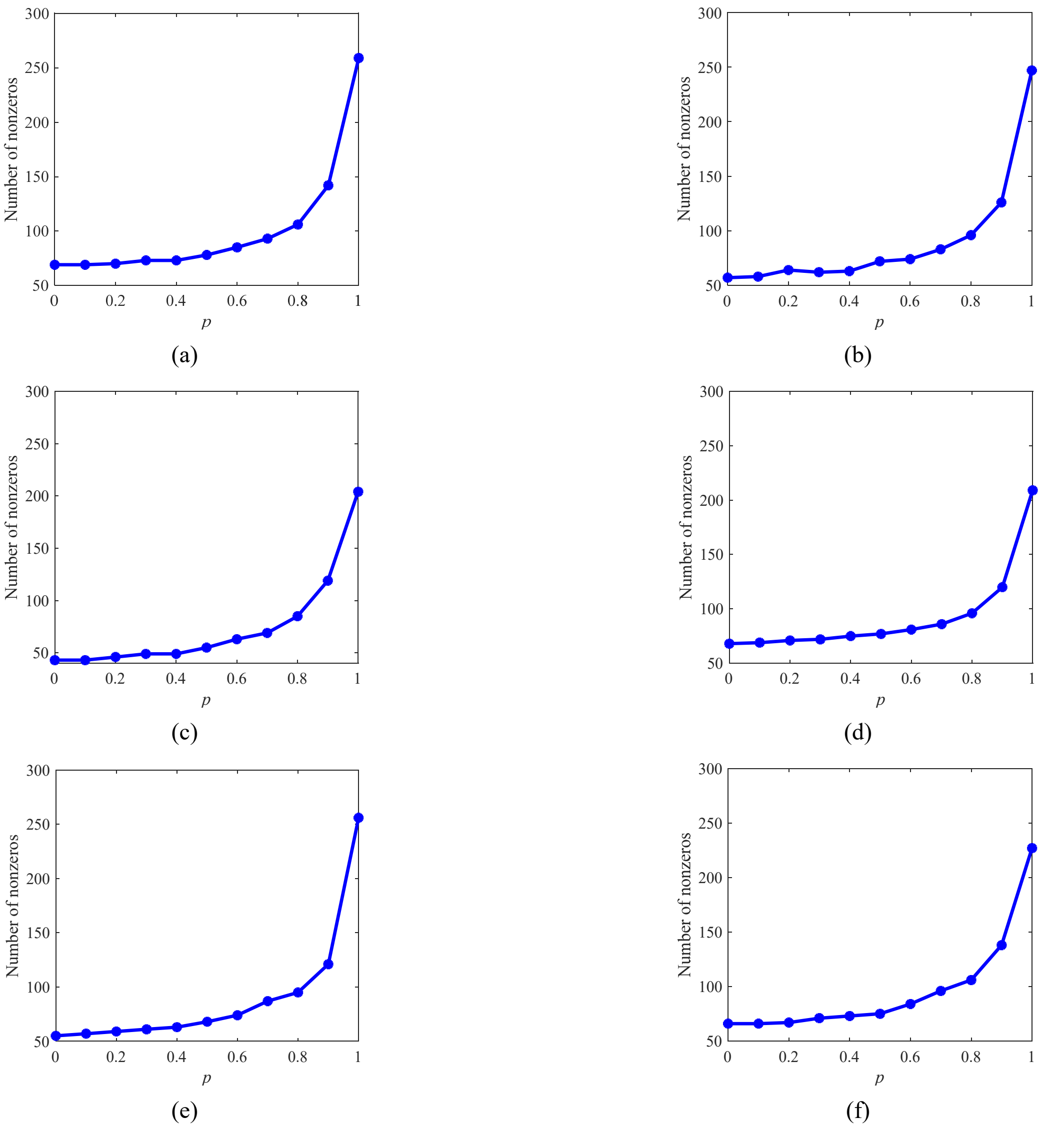

Fig. 13 The number of nonzero components in identified single impact force acting on location 5# using l_p-norm regularization as a function of p from six acceleration responses: (a) R1; (b) R2; (c) R3; (d) R4; (e) R5; and (f) R6

peak values of the $l_{1/2}$-norm solutions using acceleration responses **R1-R6** are 80.63 N, 76.95 N, 75.64 N, 79.81 N, 80.71 N, 81.45 N, respectively. The corresponding peak relative errors are only 0.71%, 5.25%, 6.86%, 1.72%, 0.62%, and -0.30%. The mildly overestimated solution of the acceleration response R6 can be attributed to uncertain measurement noise and/or modeling error. There may exist slight differences of impact locations when the transfer function matrix and the response are separately measured. Hence, the l_p-norm solutions with acceptable accuracy show excellent agreement with the reference one, the differences of which are hardly observed in Fig. 11.

Fig. 12 shows that no matter what value of p is selected, l_p-norm regularization remarkably outperforms l_1-norm regularization in reconstructing the impact force from limited measurements. l_p-norm regularization consistently reduces peak relative errors by at least 50% compared to l_1-norm regularization. Remarkably, even a value of p slightly less than 1 (e.g., p = 0.9) can yield a more accurate reconstruction of the impact force. The location of the identified impact forces using l_1-norm regularization is well localized, while their amplitudes are generally underestimated. For example, when R3 is used in Fig. 12(c), the peak relative error of the l_1-norm solution is more than 20%. Actually, the identification accuracy of each acceleration response is different. For example, the responses at plate tip (e.g., R1 and R4) are inversely used to yield more accurate solutions. The peak relative errors of the measured responses (e.g., R2 and R3) are more than 5%. One possible explanation is that the response at R3 contains less information about the impact force at a certain frequency than the responses at other locations does (Martin and Doyle 1996, Inoue *et al*. 2001). As a result, the impact force estimated from the acceleration response R3 is worse.

Compared with l_1-norm regularization, l_p-norm regularization for $0 \leq p < 1$ has a dramatic decrease in the peak relative error of the identified impact force. As previously mentioned in Section 5, on the one hand, reducing p below 1 clearly reduces the peak relative error of the identified impact force, and the reconstruction improvement is nearly monotonic in p. On the other hand, there are almost no significant improvements for p much below 1/2. For example, when R2 is used in Fig. 12(b), the peak relative error is a monotonically decreasing function as p; when R5 is used in Fig. 12(e), the best choice of p is p = 0.6. As results shown in Section 5, l_0-norm regularization with IRL1 cannot always achieve the most accurate solution.

Moreover, compared with l_1-norm regularization, l_p-norm regularization consistently has much higher sparsity as shown in Fig. 13. For a fixed p, the sparsity level of all the l_p-norm solutions using different acceleration responses is close. As $p \to 1$, the improvements of accuracy and sparsity diminish. In all, l_p-norm regularization gives much sparser and more accurate recovery results than l_1-norm regularization does. Note that although the locations #2 and #5 among nine points available are taken for example to validate the proposed method, other impact points can also generate the similar results.

6.3 Double-source impact force identification

We proceed with the experimental investigation of the circumstances under which the double-source impact forces forces acting on nine possible locations are localized and reconstructed by l_p-norm ($0 \leq p \leq 1$) regularization from six different responses. Actually, the number of actual excitation locations does not have to be known in advance. The same procedure as in Section 6.2 is performed for a different excitation configuration. The identified results of $l_{1/2}$-norm regularization using six acceleration responses are summarized in Fig. 14. $l_{1/2}$-norm regularization accurately identifies both the magnitude and location of two impact forces on locations 2# and 5#. The first impact event acting on location #2 happens at t = 0.04639 s and the second impact event acting on location #5 happens at t = 0.39400 s. The actual time delay between the two impact forces is 0.34761 s. The time histories of reconstructed impact forces using $l_{1/2}$-norm regularization match the exact ones pretty well. The difference of each acceleration response in estimating the peak force value cannot be distinguished from Fig. 14.

Fig. 15 shows the peak relative error between the measured and the identified impact forces using l_p-norm regularization as a function of p. One can find that the l_p-norm solutions with $0 \leq p < 1$ are always much more accurate than the l_1-norm solutions which greatly underestimate the peak force. l_1-norm regularization fails to provide a desired solution, when R2 and R3 are used in Figs. 15(b) and (c). As results above, even if p is slightly

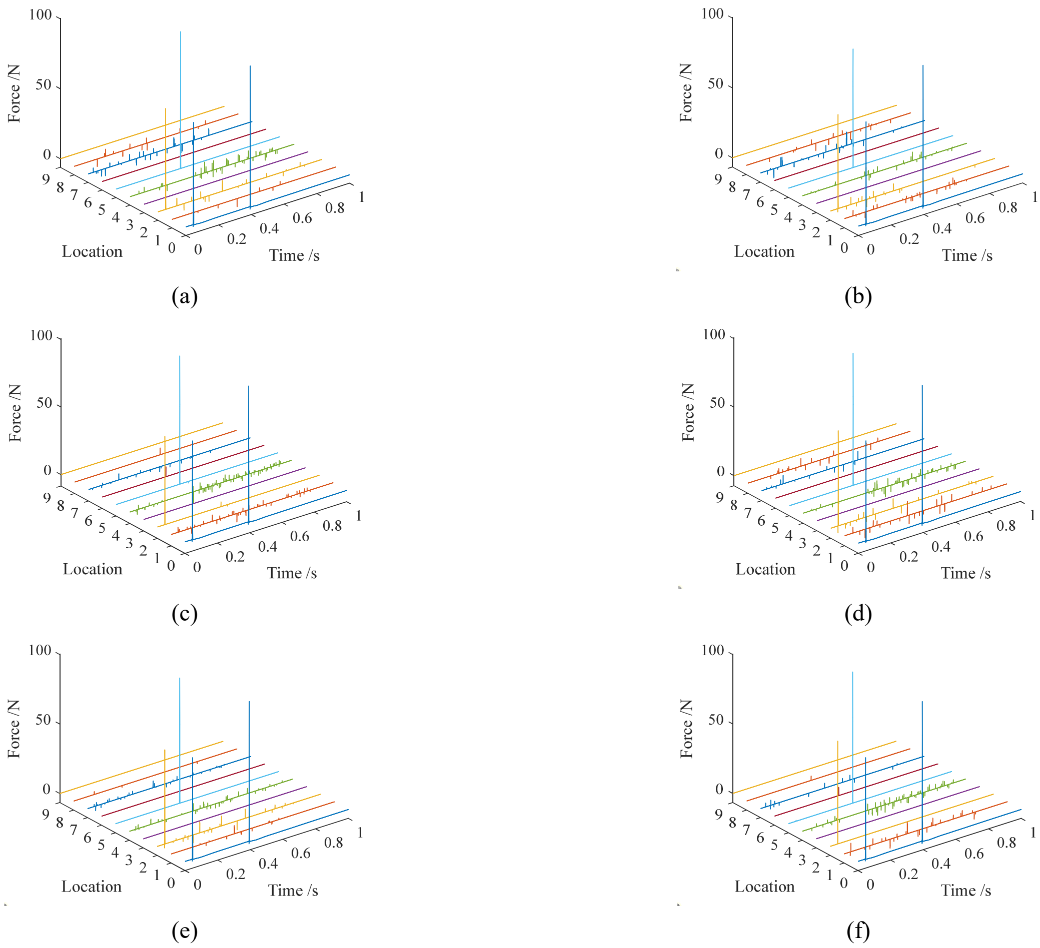

(a) (b) (c) (d) (e) (f)

Fig. 14 $l_{1/2}$-norm regularization for identifying the double-source impact forces acting on locations 2# and 5# from six acceleration responses: (a) R1; (b) R2; (c) R3; (d) R4; (e) R5; and (f) R6

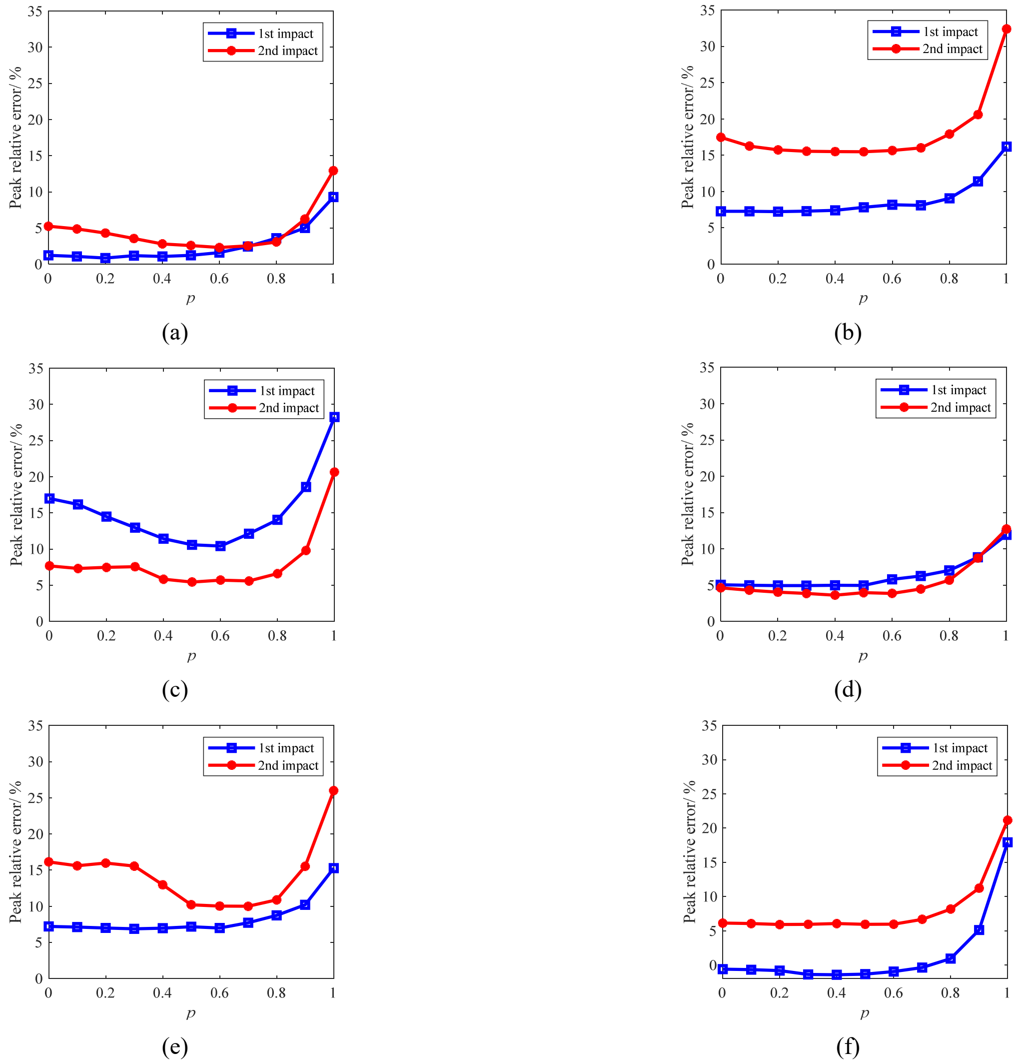

Fig. 15 The peak relative error of identified two impact forces acting on locations 2# and 5# using l_p-norm regularization as a function of p from six acceleration responses: (a) R1; (b) R2; (c) R3; (d) R4; (e) R5; and (f) R6

less than 1 (e.g., the case p = 0.9), l_p-norm regularization can significantly improve the estimation of the two impact forces. Meanwhile, it can be observed from Fig. 15 that l_p-norm regularization always generates much sparser solutions than l_1-norm regularization dose under different responses. Although different responses result in different sparse solutions, no notifiable differences in sparsity are noticed, particularly when $0 \leq p \leq 1/2$. l_p-norm regularization does remarkably outperform the standard l_1-norm regularization in accuracy and sparsity. It is the intuition that decreasing p yields the improvements of the reconstruction accuracy of impact force. Here, it is not true for the under-determined problem of double-source impact force identification. Figs. 15(a), (c) and (e) show that the peak relative error has the smallest one for $0.4 \leq p \leq 0.8$. Figs. 15(b), (e) and (f) show that when p is relatively small (e.g., $p \leq 0.6$), the peak relative error of each p is quite comparable. Actually, not all these values of p are necessarily used. Furthermore, Fig. 16 shows the number of nonzero components of the identified double-source impact forces using l_p-norm regularization. The smaller p is, the sparser the l_p-norm solutions are. Meanwhile, whenever $0 \leq p \leq 1/2$, the sparsity of l_p-norm regularization has no significant differences.

To summarize, the results of the above experiments highlight the necessity of using l_p-norm ($0 \leq p < 1$) regularization for improving the performance of impact force identification. The l_p-norm solutions are much sparser and more accurate than the l_1-norm solutions. l_p-norm regularization with IRL1 is robust with respect to the choice of the parameter p. When $0 \leq p \leq 1/2$, there are no significant differences in reconstruction performance of l_p-norm regularization. When $p \to 1$, the accuracy and sparsity of l_p-norm regularization become much worse. The preferred value p = 1/2 is taken as the representative of l_p-norm regularization. Numerical experiments (Chartrand and Staneva 2008) demonstrated that the signal sparse recovery using l_p-norm minimization is surprisingly flat for $p < 1/2$. This is also consistent with the results of $l_{1/2}$-norm regularization in Xu's work (Xu *et al.* 2012). As mentioned in Section 5, the errors of the identified single-source impact force are smaller and their results are sparser, when compared with those of the identified double-source impact forces.

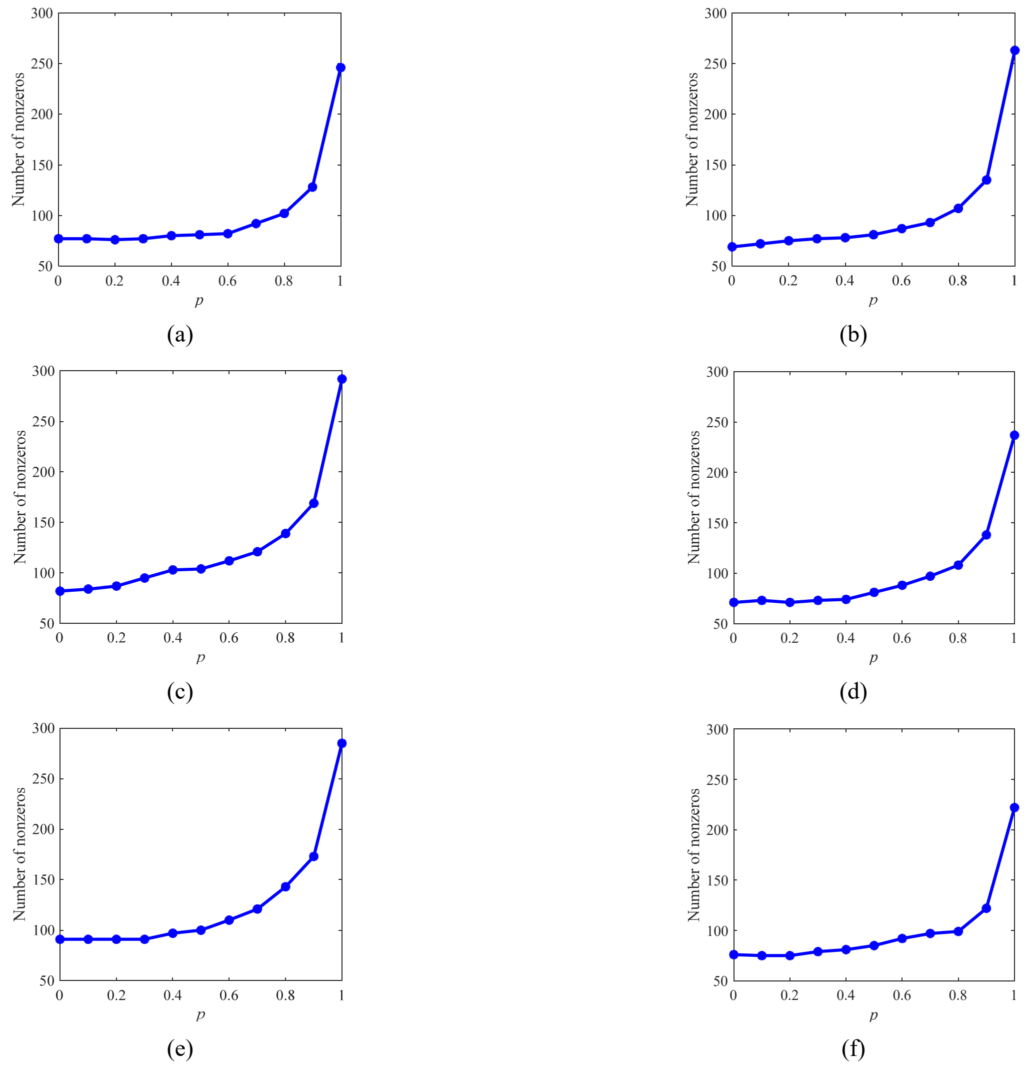

Fig. 16 The number of nonzero components in identified two impact forces acting on locations 2# and 5# using l_p-norm regularization as a function of p from six acceleration responses: (a) R1; (b) R2; (c) R3; (d) R4; (e) R5; and (f) R6

7. Conclusions

In summary, this paper presents a nonconvex l_p-norm ($0 \le p < 1$) regularization approach for the localization and simultaneous reconstruction of impact forces applied to a structure from highly incomplete measurements. We implement the l_p-norm regularization model of impact force identification by the iteratively reweighted l_1-norm minimization algorithm, in which the nonconvex problem is transferred into a series of standard l_1-norm regularization problems. Both simulation and experimental results, including the identification of single-source and double-source impact forces, demonstrate that l_p-norm regularization with $0 \le p < 10$ consistently provides more accurate and sparser solutions compared to standard l_1-norm regularization. l_p-norm regularization also outperforms l_1-norm regularization in improving the peak force amplitude. Therefore, l_p-norm regularization represents a superior alternative to l_1-norm regularization for impact force identification and can be viewed as a generalization of sparse regularization. For the highly under-determined inverse problem of impact force identification, l_p-norm regularization with IRL1 successfully localizes the impact force and simultaneously reconstructs the force time-history from a large number of possible impact locations using a single acceleration response. It should be noted that the number of actual excitation locations does not have to be known in advance. The sparse solution of the under-determined problem of impact force identification using l_p-norm regularization is very close to the actual one. Numerical examples conducted on the simply supported plate show that l_p-norm regularization is robust in finding sparse and accurate solutions of impact force in the presence of high-level noise. Experimental examples on the cantilever plate demonstrate that l_p-norm regularization can successfully identify the single and double impact forces from different acceleration responses and thus is not very sensitive to the location of sensors. In the same situations, the accuracy of the identified single-source impact force is higher than that of the identified double-source impact forces. In general, as p is approaching 0, l_p-norm regularization is closer to l_0-norm regularization. Nevertheless, it does not mean that the solution of l_0-norm regularization implemented by IRL1 is the sparsest and most accurate one. Indeed, when $0 \leq p \leq 1/2$, the peak relative error and the number of nonzero components have no significant differences. Consequently, a general suggestion is that $l_{1/2}$-norm regularization can be selected as the representative of l_p-norm ($0 \leq p \leq 1$) regularization for solving the under-determined problem of impact force identification.

Acknowledgments

This work is supported by National Natural Science Foundation of China (Nos. 52305127 & 52075414), and China Postdoctoral Science Foundation (No.2021M702595).

References

Candes, E.J., Wakin, M.B. and Boyd, S.P. (2008), "Enhancing sparsity by reweighted ℓ1 minimization", *J. Fourier Anal. Appl.*, **14**(5), 877-905. https://doi.org/10.1007/s00041-008-9045-x

Chartrand, R. (2007), "Exact reconstruction of sparse sig-nals via nonconvex minimization", *IEEE Signal Proc. Let.*, **14**(10), 707-710. https://doi.org/10.1109/LSP.2007.898300

Chartrand, R. and Staneva, V. (2008), "Restricted isometry properties and nonconvex compressive sensing", *Inverse Probl.*, **24**(3), 035020. https://doi.org/10.1088/0266-5611/24/3/035020

Chen, Y., Joffre, D. and Avitabile, P. (2018), "Underwater dynamic response at limited points expanded to full-field strain response", *J. Vib. Acoust.*, **140**(5), 051016. https://doi.org/10.1115/1.4039800

Donoho, D.L. (2006), "For most large underdetermined sys-tems of linear equations the minimal ℓ1-norm solution is also the sparsest solution", *Commun. Pur. Appl. Math.*, **59**(6), 797-829. https://doi.org/10.1002/cpa.20132

Foucart, S. and Lai, M.J. (2009), "Sparsest solutions of un-derdetermined linear systems via ℓq-minimization for 0 < q⩽ 1", *Appl. Comput. Harmon. A.*, **26**(3), 395-407. https://doi.org/10.1016/j.acha.2008.09.001

Inoue, H., Harrigan, J.J. and Reid, S.R. (2001), "Review of inverse analysis for indirect measurement of impact force", *Appl. Mech. Rev.*, **54**(6), 503-524. https://doi.org/10.1115/1.1420194

Jacquelin, E., Bennani, A. and Hamelin, P. (2003), "Force reconstruction: analysis and regularization of a decon-volution problem", *J. Sound Vib.*, **265**(1), 81-107. https://doi.org/10.1016/S0022-460X(02)01441-4

Kalhori, H., Alamdari, M.M. and Ye, L. (2018), "Automated algorithm for impact force identification using cosine similarity searching", *Measurement*, **122**, 648-657. https://doi.org/10.1016/j.measurement.2018.01.016

Khoo, S.Y., Ismail, Z., Kong, K.K., Ong, Z.C., Noroozi, S., Chong, W.T. and Rahman, A.G.A. (2014), "Impact force identification with pseudo-inverse method on a light-weight structure for under-determined, even-determined and over-determined cases", *Int. J. Impact Eng.*, **63**, 52-62. https://doi.org/10.1016/j.ijimpeng.2013.08.005

Koh, K., Kim, S.J. and Boyd, S. (2007), "An interior-point method for large-scale l1-regularized logistic regression", *J. Mach. Learn. Res.*, **8**, 1519-1555.

Lai, M. and Wang, J. (2011), "An Unconstrained lq Minimization with 0 < q ≤ 1 for Sparse Solution of Underdeter-mined Linear Systems", *SIAM J. Optimiz.*, **21**(1), 82-101.

Li, Q. and Lu, Q. (2018), "A hierarchical Bayesian method for vibration-based time domain force reconstruction problems", *J. Sound Vib.*, **421**, 190-204. https://doi.org/10.1016/j.jsv.2018.01.052

Liu, J., Sun, X., Han, X., Jiang, C. and Yu, D. (2014), "A novel computational inverse technique for load identifi-cation using the shape function method of moving least square fitting", *Comput. Struct.*, **144**, 127-137. https://doi.org/10.1016/j.compstruc.2014.08.002

Liu, J., Qiao, B., He, W., Yang, Z. and Chen, X. (2020), "Impact force identification via sparse regularization with generalized minimax-concave penalty", *J. Sound Vib.*, **484**, 115530. https://doi.org/10.1016/j.jsv.2020.115530

Liu, J., Qiao, B., Chen, Y., Zhu, Y., He, W. and Chen, X. (2022), "Impact force reconstruction and localization using nonconvex overlapping group sparsity", *Mech. Syst. Signal Process.*, **162**, 107983. https://doi.org/10.1016/j.ymssp.2021.107983

Liu, J., Qiao, B., Wang, Y., He, W. and Chen, X. (2023), "Non-convex sparse regularization via convex optimiza-tion for impact force identification", *Mech. Syst. Signal Prcess.*, **191**, 110191. https://doi.org/10.1016/j.ymssp.2023.110191

Mahzan, S., Staszewski, W.J. and Worden, K. (2010), "Ex-perimental studies on impact damage location in compo-site aerospace structures using genetic algorithms and neural networks", *Smart Struct. Syst., Int. J.*, **6**(2), 147-165. https://doi.org/10.12989/sss.2010.6.2.147

Martin, M.T. and Doyle, J.F. (1996), "Impact force identification from wave propagation responses", *Int. J. Impact Eng.*, **18**(1), 65-77. https://doi.org/10.1016/0734-743X(95)00022-4

Pan, C.D., Yu, L., Liu, H.L., Chen, Z.P. and Luo, W.F. (2018), "Moving force identification based on redundant concatenated dictionary and weighted l1-norm regularization", *Mech. Syst. Signal Process.*, **98**, 32-49. https://doi.org/10.1016/j.ymssp.2017.04.032

Park, J., Ha, S.F. and Chang, K. (2009), "Monitoring impact events using a system-identification method", *AIAA J.*, **47**(9), 2011-2021. https://doi.org/10.2514/1.34895

Qiao, B., Zhang, X., Gao, J., Liu, R. and Chen, X. (2016a), "Impact-force sparse reconstruction from highly incomplete and inaccurate measurements", *J. Sound Vib.*, **376**, 72-94. https://doi.org/10.1016/j.jsv.2016.04.040

Qiao, B., Zhang, X., Wang, C., Zhang, H. and Chen, X. (2016b), "Sparse regularization for force identification using dictionaries", *J. Sound Vib.*, **368**, 71-86. https://doi.org/10.1016/j.jsv.2016.01.030

Qiao, B., Zhang, X., Gao, J., Liu, R. and Chen, X. (2017), "Sparse deconvolution for the large-scale ill-posed inverse problem of impact force reconstruction", *Mech. Syst. Signal Process.*, **83**, 93-115. https://doi.org/10.1016/j.ymssp.2016.05.046

Qiao, B., Liu, J., Liu, J., Yang, Z. and Chen, X. (2019), "An enhanced sparse regularization method for impact force identification", *Mech. Syst. Signal Process.*, **126**, 341-367. https://doi.org/10.1016/j.ymssp.2019.02.039

Qiao, B., Ao, C., Mao, Z. and Chen, X. (2020a), "Non-convex sparse regularization for impact force identification", *J. Sound Vib.*, **477**, 115311. https://doi.org/10.1016/j.jsv.2020.115311

Qiao, B., Mao, Z., Sun, H., Chen, S. and Chen, X. (2020b), "Sparse reconstruction of guided wavefield from limited measurements using compressed sensing", *Smart Struct. Syst., Int. J.*, **25**(3), 369-384. https://doi.org/10.12989/sss.2020.25.3.369

Qiu, L. and Yuan, S. (2011), "A phase synthesis time reversal impact imaging method for on-line composite structure monitoring", *Smart Struct. Syst., Int. J.*, **8**(3), 303-320. https://doi.org/10.12989/sss.2011.8.3.303

Saleem, M.M. and Jo, H. (2019), "Impact force localization for civil infrastructure using augmented Kalman Filter optimization", *Smart Struct. Syst., Int. J.*, **23**(2), 123-139. https://doi.org/10.12989/sss.2019.23.2.123

Selesnick, I.W. and Bayram, I. (2014), "Sparse signal estimation by maximally sparse convex optimization", *IEEE Trans. Signal Process*, **62**(5), 1078-1092. https://doi.org/10.1109/TSP.2014.2298839

Thite, A.N. and Thompson, D.J. (2003), "The quantification of structure-borne transmission paths by inverse methods. Part 2: Use of regularization techniques", *J. Sound Vib.*, **264**(2), 433-451. https://doi.org/10.1016/S0022-460X(02)01203-8

Wambacq, J., Maes, K., Rezayat, A., Guillaume, P. and Lombaert, G. (2019), "Localization of dynamic forces on structures with an interior point method using group sparsity", *Mech. Syst. Signal Process.*, **115**, 593-606. https://doi.org/10.1016/j.ymssp.2018.06.006

Wipf, D. and Nagarajan, S. (2010), "Iterative Reweighted l1 and l2 methods for finding sparse solutions", *IEEE J-STSP*, **4**(2), 317-329.

Xu, Z., Chang, X. Xu, F. and Zhang, H. (2012), "L1/2 regularization: A thresholding representation theory and a fast solver", *IEEE T. Neur. Net. Lear.*, **23**(7), 1013-1027. https://doi.org/10.1109/TNNLS.2012.2197412

Yan, G., Sun, H. and Buyukozturk, O. (2017), "Impact load identification for composite structures using Bayesian regularization and unscented Kalman filter", *Struct. Control Health Monitor.*, **24**(5), e1910. https://doi.org/10.1002/stc.1910

Zhong, Y. and Xiang, J. (2016), "A two-dimensional plum-blossom sensor array-based multiple signal classi-fication method for impact localization in composite structures", *Comput.-Aided Civil Infrastr. Eng.*, **31**(8), 633-643. https://doi.org/10.1111/mice.12198

Zhong, Y. and Xiang, J. (2019), "Impact location on a stiffened composite panel using improved linear array", *Smart Struct. Syst., Int. J.*, **24**(2), 173-182. https://doi.org/10.12989/sss.2019.24.2.173

Zhou, R., Wang, Y., Qiao, B., Zhu, W., Liu, J. and Chen, X. (2024), "Impact force identification on composite panels using fully overlapping group sparsity based on L_p-norm regularization", *Struct Health Monitor.*, **23**(1), 137-161. https://doi.org/10.1177/1475921723116570